

The role of Fjx1 in the repair of toxic renal injury in an ADPKD mouse model



Leids Universitair Medisch Centrum

Maaïke Heidinga

Biology and Medical laboratory science

University of Applied Sciences Leiden

18-05-2016

The role of Fjx1 in the repair of toxic renal injury in an ADPKD mouse model

Graduate thesis

Name: Maaïke Heidinga
Student nr: 1080442
Date: 18-5-2016

School: University of Applied Sciences Leiden
Programme: Biology and Medical laboratory science
Specialization: Cytohistopathology
Mentor: dr. A. Tiggelman

Graduation place: Leids Universitair Medisch Centrum
Albinusdreef 2
2333 ZA Leiden
Departments: Pathology and Human Genetics
Supervisors: Dr. M. Scharpfenecker, C. Formica Msc,
K.A.M. Veraar Bsc
Period: 1-10-2015 until 31-5-2016

Signature supervisor:

Abstract

De erfelijke ziekte ADPKD (autosomaal dominant polycysteuze nierziekte) wordt gekenmerkt door het ontstaan van renale cystes. Deze cystes worden veroorzaakt door een aangeboren mutatie in het *Pkd1*- of *Pkd2*-gen (polycystic kidney disease-1 of 2 gen). Deze genen coderen voor eiwitten die bijdragen aan regulatie van proliferatie, differentiatie en apoptose. Na een aanvullende somatische mutatie kunnen epitheliale niercellen cystes gaan ontwikkelen, die vervolgens schade in het weefsel veroorzaken en het ontstaan van meer cystes induceren. Dit leidt uiteindelijk tot nierfalen.

Uit een studie van Happé (2009) naar de cystogenese in een *Pkd1* KO muismodel, is het gen *Four jointed box 1* (*Fjx1*) naar voren gekomen als kandidaat voor verder onderzoek. Gedacht wordt aan een mogelijke rol van *Fjx1* in het herstelproces na schade binnen de pathogenese van ADPKD.

Om deze hypothese te onderzoeken is een experiment met verschillende C57Bl/6J knockout (KO) muizen opgezet. Hierbij is een *Fjx1*^{-/-};*Pkd1* KO model vergeleken met een *Pkd1* KO model. Als controles zijn *Fjx1*^{-/-}- en wild type (WT) muizen meegenomen. Alle modellen hebben het nefrotoxine S-(1,2-dichlorovinyl)-L-cysteïne (DCVC) toegediend gekregen om schade te induceren en cysteformatie te versnellen, terwijl aan controlemuizen PBS toegediend is. De muizen zijn op 1, 2, 5, en 10 weken na DCVC-toediening en bij nierfalen (gedefinieerd als bloed ureumlevel >25mmol/l) opgeofferd.

Voor het *Pkd1* KO model geldt dat na toediening van DCVC eerder nierfalen optrad dan bij muizen die PBS kregen toegediend. Bij de *Fjx1*^{-/-};*Pkd1* KO muizen trad echter gelijktijdig nierfalen op in zowel de DCVC- als de PBS-muizen.

Om dit verschil te verklaren zijn diverse parameters gemeten. De hoeveelheid cystevorming is bepaald met de cyste-index. Daarnaast is de hoeveelheid fibrose bepaald met de fibrose-index als resultante van het reparatieproces. De mate van nierschade is bepaald met de schademarkers Lipocalin-2. Omdat DCVC-geïnduceerde schade op 36 uur na toediening op zijn hoogtepunt is, is tevens een pilot opgezet waarbij *Fjx1*^{-/-};*Pkd1* KO muizen en *Pkd1* KO muizen op 24, 48 en 72 uur na DCVC-toediening zijn opgeofferd. Hierbij is, naast bepaling van de nierschade, de hoeveelheid proliferatie met behulp van een BrdU-kleuring bepaald.

Uit de resultaten blijkt dat er geen significante verschillen zijn tussen de *Fjx1*^{-/-};*Pkd1* KO muizen en de *Pkd1* KO muizen, als gekeken werd naar de hoeveelheid cystes en fibrose. Wel lijkt de hoeveelheid schade voor de *Fjx1*^{-/-};*Pkd1* KO muizen lager te zijn dan voor de *Pkd1* KO muizen. Voor de pilotmuizen komt de hoeveelheid proliferatie in de verschillende muismodellen met elkaar overeen. Om de rol van *Fjx1* op celniveau te onderzoeken zijn twee *Fjx1*-knockout collecting ducts cellijnen vergeleken met een WT cellijn, waarbij is gekeken naar celmorfologie en groeisnelheid. Wat betreft morfologie komen de *Fjx1*-knockout cellijnen overeen met de WT cellijn, maar de groeisnelheid is verlaagd in vergelijking met de WT cellijn.

Concluderend verschillen de DCVC-*Fjx1*^{-/-};*Pkd1* KO muizen en DCVC-*Pkd1* KO muizen van elkaar wat betreft het moment van optreden van nierfalen. Dit kan niet worden toegeschreven aan een verschil in hoeveelheid cystes, fibrose, schade of proliferatie. Om de oorzaak van dit verschil te vinden, is aanvullend onderzoek nodig.

Table of Contents

Abstract.....	4
List of abbreviations.....	7
Introduction	8
Material and methods	13
Mouse models.....	13
qPCR.....	13
RNA isolation.....	13
Generating cDNA	13
qPCR.....	13
Analysis	14
Histology	14
General.....	14
PAS staining.....	14
Cystic index (CI).....	14
Sirius Red staining.....	15
Fibrotic Index (FI)	15
Immunohistochemistry.....	15
Lipocalin-2 staining	15
Lipocalin-2 analysis	16
BrdU staining.....	16
BrdU analysis.....	16
Cell culture	17
Morphology.....	17
Growth curve	17
Wound healing.....	17
Results.....	19
<i>Fjx1</i> expression is increased in WT mice compared to <i>Pkd1</i> KO mice at the 10 week time point ...	19
<i>Pkd1</i> KO and <i>Fjx1</i> ^{-/-} ; <i>Pkd1</i> KO mice show an increased cystic index at 10 weeks and failure time points	19
<i>Fjx1</i> ^{-/-} ; <i>Pkd1</i> KO mice show slightly less damage compared to <i>Pkd1</i> KO mice.....	21
Early time points <i>Fjx1</i> ^{-/-} ; <i>Pkd1</i> KO mice show no difference in proliferation compared to <i>Pkd1</i> KO mice.....	23
<i>Fjx1</i> ^{-/-} ; <i>Pkd1</i> KO mice show no relevant differences in fibrotic index compared to <i>Pkd1</i> KO mice ...	24
Characterization of <i>Fjx1</i> KO cell lines.....	26

<i>Fjx1</i> KO cells appear to have the same morphology compared to WT cells.....	26
WT cells have a higher growth rate compared to <i>Fjx1</i> KO cells.....	27
Wound healing.....	27
Discussion and conclusion	29
References	33
Appendices.....	35
1 PCP pathway	35
2 Background mouse models.....	36
3 Preliminary results	37

List of abbreviations

ADPKD	autosomal dominant polycystic kidney disease
BrdU	bromodeoxyuridine
BSA	Bovine Serum Albumin
CI	cystic index
DCVC	1,2-dichlorovinylcystein
EDTA	ethylenediaminetetraacetic acid
FI	fibrotic index
<i>Fjx1</i>	<i>Four Jointed Box 1</i>
<i>Fjx1</i> ^{-/-}	<i>Fjx1</i> knockout mouse
<i>Fjx1</i> ^{-/-} ; <i>Pkd1</i> KO	double <i>PKD1/Fjx1</i> knockout mouse
GOI	gene of interest
HPRT	Hypoxanthine-guanine phosphoribosyltransferase
PBS	Phosphate Buffered Saline
PBST	Phosphate Buffered Saline with Tween20
PCP	planar cell polarity
PC1	polycystin-1
PC2	polycystin-2
<i>Pkd1</i> KO	<i>Pkd1</i> knockout mouse
<i>Pkd1</i>	polycystic kidney disease-1
<i>Pkd2</i>	polycystic kidney disease-2
YAP	Yes-Associated Protein
WT	wild type

Introduction

Autosomal dominant polycystic kidney disease (ADPKD) is an inheritable disease with a prevalence of approximately 4:10.000 in the region south west Germany.¹ Its main hallmark is the formation of renal fluid-filled cysts. It is additionally characterized by cyst formation in the liver and pancreas, as well as cardiovascular abnormalities. Some of the symptoms that can occur are enlarged kidneys, hypertension, pain, sleep disturbance, heartburn and fever.²

No definitive treatment has been found so far,^{2,3} although recently a drug called Tolvaptan was approved for treatment. This Vasopressin V₂-receptor antagonistic drug can slow down the progression of ADPKD.⁴

A known important contributor in ADPKD is the polycystic kidney disease - 1 (*Pkd1*) gene, encoding for the polycystin-1 (PC1) protein. This gene is mutated in 85% of the ADPKD-cases. In the remaining 15% of the cases, a mutation of the polycystic kidney disease -2 (*Pkd2*) gene, encoding for the polycystin-2 (PC2) protein, is involved.⁵ This latter mutation is associated with a less severe clinical course, due to development of a lower number of cysts early in life. A mutation in one of these genes is a necessary, but not sufficient condition for the onset of ADPKD.

As was mentioned in the previous paragraph, the *Pkd1* and *Pkd2* genes encode for respectively PC1 and PC2. The PC1 protein is a transmembrane glycoprotein. It functions as a receptor and adhesion molecule, managing cell-cell and cell-ECM (extracellular matrix) interactions. Its expression is highest in the developing kidney.^{3,6}

PC2 is also a transmembrane glycoprotein and serves as a non-selective cation channel, permeable for Ca²⁺. Its activity is regulated by PC1 in a polycystin-signaling complex of PC1 and PC2, which is located mainly in the cilia. It functions as a mechano- or chemosensor, providing information for the appropriate growth direction. The complex converts extracellular stimuli in Ca²⁺ influx into the cell; this triggers Ca²⁺ release from intracellular stores, thereby modulating several signaling pathways which regulate, amongst others, cell proliferation, differentiation and apoptosis.^{3,6}

During pathogenesis (shown in figure 1), all renal tubular epithelial cells contain a normal allele and an inherited allele with a *Pkd1* or *Pkd2* mutation. Different mutations, for example complete loss of the gene, point mutations or deletions can result in either absent or aberrant protein. An additional event is required for cells to become cystic. This additional event is thought to be either a "second hit mutation" in the normal allele of *Pkd1* or *Pkd2*, or a fluctuation in *Pkd1* or *Pkd2* gene dosage. Due to hyperproliferation and altered fluid transport, cysts will grow and expand. Once formed, the cysts impose continuous stress onto the surrounding tissue and the resulting injury triggers additional cyst formation. In the final stage of the disease, apoptosis, fibrosis and infiltration of inflammatory cells occur which leads to the decline of renal function. At this point kidney dialysis or transplantation is required. The process of pathogenesis can be accelerated by renal damage, producing additional growth factors and inflammation. There are multiple hypotheses regarding the underlying mechanism of accelerated pathogenesis. One of those hypotheses, for example, suggests that renal injury in the absence of PC1 or PC2 will lead to aberrant tissue repair, which might be the cause of more altered cell integrity and a faster disease progression.³

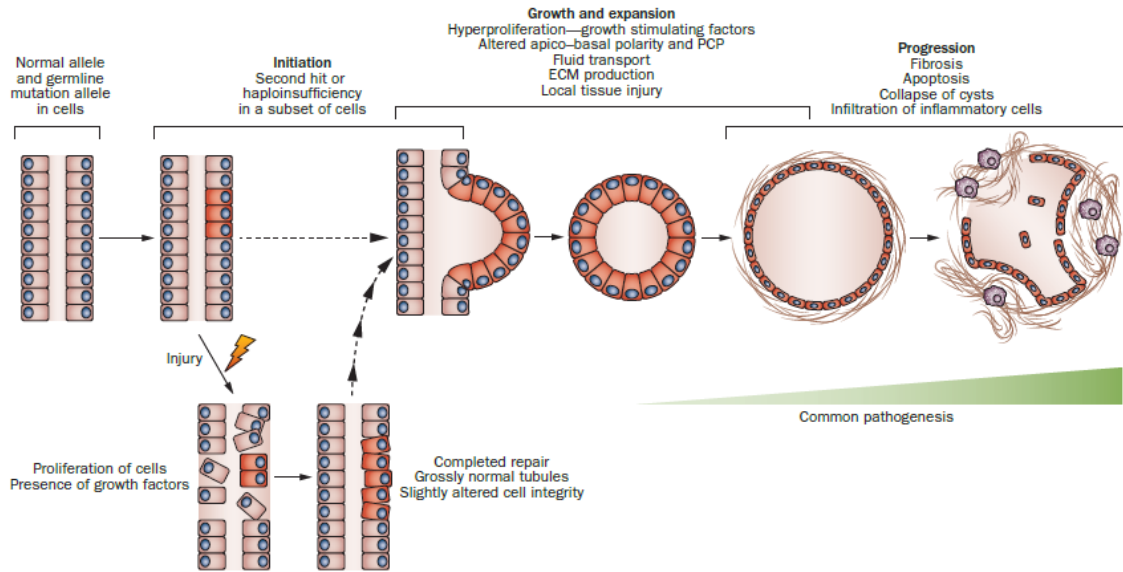


Figure 1. Pathogenesis of ADPKD³

One of the signalling pathways involved in the pathogenesis of ADPKD is the Planar Cell Polarity (PCP) pathway³ (shown in appendix 1), which is also referred to as the non-canonical Wnt signalling pathway.³ This pathway is influenced by PC1⁵ and it is a regulator of the PCP.³ PCP is a mechanism in the development of spatial structures. Epithelial cells show an apical-basal polarity, which helps them in oriented cell division in a vertical plane. Orthogonally to this axis, a planar polarity is shown, directing the cell into a correctly oriented cell division in the horizontal plane⁸ (shown in figure 2).

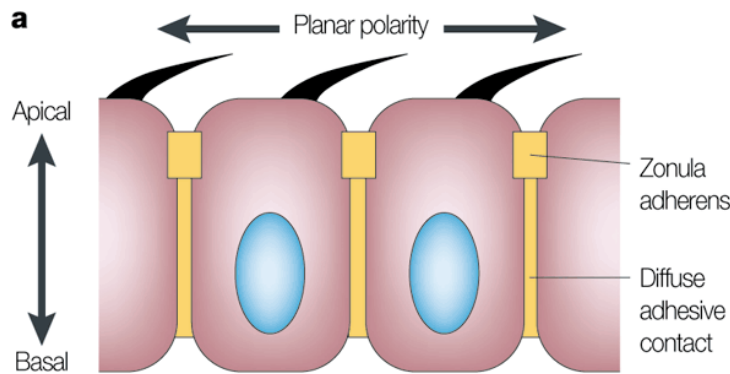


Figure 2. Orientation in a horizontal plane is called planar cell polarity. The black “hairs” are the cilia containing the PC1/PC2 complex.⁹

A disturbed PCP is known to be involved in development of polycystic kidneys.¹⁰ Indeed, loss of the PCP gene *Fat4* leads to cyst formation in the kidney.¹¹

The regulation of PCP is very complex and many routes have been described. Another group of regulators in the PCP consists of a complex of three proteins: Fat (Ft), Dachshous (Ds) and Four jointed (Fjx1). Fjx1 is a Golgi kinase which can phosphorylate the extracellular domains of Ft and Ds and therefore can activate or block the PCP pathway.^{10,11} This process is shown in figure 3.¹²

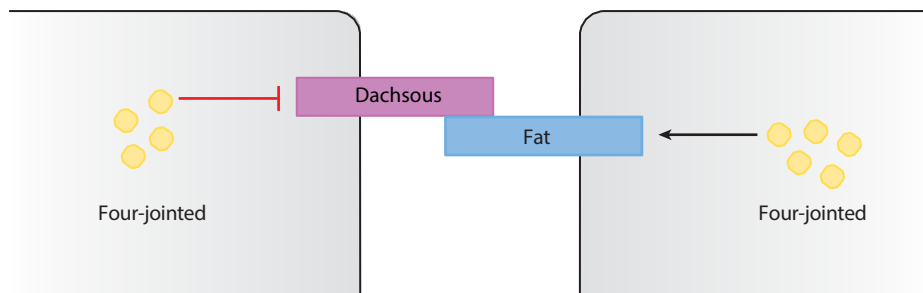


Figure 3. Phosphorylation of Fat by Fjx1 improves binding of Fat and Dachsous. If Dachsous is phosphorylated by Fjx1, binding is inhibited.

Happé et al. (2009) investigated expression of several genes involved in PCP during their study on injury induced cystogenesis in *Pkd1* knock out (KO) mice. One of these genes was *Fjx1*, a regulator of the mentioned PCP pathway, whose location in the pathway is shown in appendix 1.^{7,13} Because of its opposite expression in a *Pkd1* KO mouse model compared to a wild type control model, it was hypothesized that *Fjx1* would be involved in tissue repair. Except for its role in the phosphorylation of Ft and Ds described above, little is known about the function of this protein and its associated gene. It is supposed to be a regulator of angiogenesis¹⁴ and is expressed in epithelial cells of multiple organs. In *Drosophila* the homologue of this gene encodes a partially secreted transmembrane glycoprotein.^{15,16} It has a gradient expression pattern, thereby giving directional information about the orientation of the cell.¹⁶

To study the role of *Fjx1* and its suspected role in tissue repair in ADPKD, four mouse models have been developed (see also appendix 3):

- *Fjx1*^{-/-} mice: *Fjx1* knockout mice
- *ikspPkd1*^{del} mice: mice with inducible kidney epithelium specific knockout for *Pkd1* (referred to as *Pkd1* KO)
- *ikspPkd1*^{del};*Fjx1*^{-/-} mice: a combination of the above genotypes: mice with *Fjx1* knockout and kidney epithelium specific inducible knockout for *Pdk1* (referred to as *Fjx1*^{-/-};*Pkd1* KO)
- *Pkd1*^{loxlox} mice: wild type mice (referred to as WT)

The *Fjx1*^{-/-};*Pkd1* KO model is used as experimental condition, while both the *Pkd1* KO and the *Fjx1*^{-/-} served as controls, just as the WT. S-(1,2-dichlorovinyl)-L-cysteine (DCVC) was administered to all mouse models to induce injury and as a result, it additionally accelerated cyst formation.¹¹ To control for this effect, PBS-administered mice were included.

At several fixed time points after injection, namely 1, 2, 5 and 10 weeks, mice were sacrificed and kidneys were collected. Kidneys were also obtained when the blood urea level exceeded 25mmol/l, because this indicates severe kidney failure and therefore the mouse was sacrificed.

To investigate the hypothesis of involvement of *Fjx1* in tissue repair, the following research questions have been drafted:

- What is the mRNA-expression pattern of *Fjx1* in the *Pkd1* KO and WT mouse models?
- What is the role of *Fjx1* in response to damage of renal epithelial cells in ADPKD mouse models?
- How can this role be explained?
 - Is there a difference in amount of cysts between *Pkd1* KO and *Fjx1*^{-/-};*Pkd1* KO mice?

- Is there a difference in amount of damage between *Pkd1* KO and *Fjx1*^{-/-};*Pkd1* KO mice?
- Is there a difference in amount of fibrosis between *Pkd1* KO and *Fjx1*^{-/-};*Pkd1* KO mice?
- What are the effects of a knockout of the *Fjx1* gene in a cell line considering morphology, growth rate and cell migration?

Our preliminary data suggest that *Fjx1*^{-/-};*Pkd1* KO mice recover faster or more effectively from damage compared to *Pkd1* KO mice, which allows them to survive longer. Therefore *Fjx1* seems to be involved in tissue repair. This is explained in more detail in appendix 4.

In continuation of these results, the following experiments will be conducted:

- As mentioned earlier, the study is based on a hypothesis of involvement of *Fjx1* in tissue repair, derived from an experiment performed by Happé et al (2009). They showed decreased *Fjx1* expression in *Pkd1* KO mice. To confirm these results, *Fjx1* expression will also be investigated by qPCR in the mouse models of the current study. In a qPCR, the amount of a specific mRNA in a sample can be determined. RNA is converted into cDNA and is subsequently used in a PCR reaction. Detection of the PCR product is done with the help of SYBR Green, a fluorescent dye, which binds to double strand DNA. During amplification of the gene of interest, SYBR Green will be incorporated into dsDNA, thereby increasing its fluorescent intensity. The amount of fluorescence can be measured and used to measure the amount of mRNA of interest. Results are normalized to the reference gene and subsequently displayed in relation to the samples of the WT 1 week mice, which were set to 1.
- One of the hallmarks of ADPKD is formation of cysts. It is known that there is a relation between the amount of cysts and kidney failure.³ The percentage of area covered by cysts in the sections will be determined, resulting in a cystic index. Because cysts will develop later in life, only mice sacrificed at 5 weeks, 10 weeks and at renal failure will be analysed. For this purpose PAS-stained sections will be used. In this histochemical staining, periodic acid oxidizes the glycol groups in carbohydrates into aldehyde groups. This is able to react with Schiff's reagent. Rinsing in tap water allows the SO₃⁻ groups to be released, which gives the carbohydrates their magenta until purple color. The PAS-stained slide nicely reflects kidney morphology and shows the brush border and the basal membrane, which contain a lot of carbohydrates. Also, PAS-stained sections have a high contrast between the lumen and the tissue, which makes the analysis easier. The analysis will be done using Photoshop, by calculating the area percentage of cyst lumen in the total section, which results in a cystic index.
- To investigate the role of *Fjx1* in the repair of renal epithelial cell damage, the amount of injury needs to be identified. To characterise the induced damage, an immunohistochemical staining for Lipocalin-2 (LCN2, also known as neutrophil gelatinase-associated lipocalin (NGAL)), will be performed. This marker for oxidative stress¹⁷ is used as a readout for kidney damage¹⁸. In immunohistochemical stainings, firstly a primary antibody specific for an antigen of interest and secondly a secondary antibody will be added to the tissues. The secondary antibody contains a HRP label, which can catalyse the oxidation of 3,3'-diaminobenzidine (DAB), which results in a dark brown color. In this way, a protein of interest (the antigen) is made visible. The staining is performed for the 1 and 2 week time points. These time points have been chosen because they are close to the peak of the damage induced by DCVC, which occurs at 36 hours post injection.¹⁹

After two weeks, most of the damage will be repaired,¹¹ thereby no or less staining will be expected at later time points. For analysis, all groups will be compared to the WT mice, while the *Pkd1* KO phenotype will be compared with the *Fjx1*^{-/-};*Pkd1* KO model. The PBS-injected mice are controls for the DCVC-injected animals, as they should have less or no renal damage. The staining will be analysed by scoring the percentage of staining on a 3-points scale. This will be done by two independent raters. Statistical analysis will be done using a non-parametrical test, because the scores don't represent values.

- As the peak of the damage occurs at 36 hours and tissue will only be obtained after one week, changes in the response to damage might be missed. Therefore, a pilot will be performed: two mice per genotype (*Fjx1*^{-/-};*Pkd1* KO and *Pkd1* KO) will be sacrificed at 24, 48 and 72 hours post DCVC injection. Two hours prior to sacrifice, bromodeoxyuridine (BrdU) will be administered. BrdU is an analogue of thymidine and will be incorporated in the DNA during proliferation. It can be immunohistochemically visualized and this will give more information about the response to damage. The amount of proliferation will be quantified using ImageJ. In this program, the amount of haematoxylin-stained nuclei can be determined, as well as the amount of DAB-stained nuclei. The percentage of DAB-stained nuclei will be calculated for the cortico-medullary region. In this region the parts of the proximal tubules, which are the first to start proliferation after damage, are located. In addition, a Lipocalin-2 staining will be performed for these early time points. Because the amount of staining is higher in comparison to the staining of the 1 and 2 week mice, a different scoring scale will be used.
- To characterise the amount of injury, tissue of the different genotypes will be scored on one of the characteristics of ADPKD, namely the onset and degree of fibrosis.²⁰ To be able to do so, sections of all time points will be stained with a Sirius Red staining. The principle of this staining is not fully understood, but it shows collagen deposition in red. Analysis of the amount of red stain in Photoshop will give a fibrotic index. This is defined as percentage of fibrosis in the total tissue. The percentage of fibrosis will be compared between the different groups and statistics will show whether differences are significant.
- To investigate the role of *Fjx1* on a cellular level, a *Fjx1* knockout cell line will be characterized for general characteristics like morphology and growth rate. Also a wound healing assay will be performed to investigate cell migration. For this purpose an established cell line will be transfected to induce a *Fjx1* knockout cell line, using a type of CRISPR/Cas9 technique called RNA-guided FokI Nuclease. In this technique, a double strand break is induced by restriction enzymes, directed by a specific DNA sequence. Repair by non-homologous end joining will result in correct repair and in incorrectly repaired, thus mutated genes. These mutated cells are used as *Fjx1* knockout cell lines. Because the transfection might have off-target events, two clones will be used to control for this.

The aim of this research is to compare the *Fjx1*^{-/-};*Pkd1* KO model with the *Pkd1* KO model, to investigate the role of *Fjx1*. The role of DCVC has been studied before and it was demonstrated that DCVC accelerates cystogenesis.³

Because the earlier mentioned preliminary findings suggest that the *Fjx1*^{-/-};*Pkd1* KO model has a faster or more effective response to injury (i.e. an earlier onset of repair or a more effective repair), it is hypothesized that a difference in fibrosis will occur between the *Pkd1* KO and *Fjx1*^{-/-};*Pkd1* KO models, since fibrosis is a result of the repair process. Besides, it is hypothesized that proliferation will take place at an earlier moment for the *Fjx1*^{-/-};*Pkd1* KO model compared to the *Pkd1* KO model.

Material and methods

Mouse models

In this experiment male C57Bl/6J mice were used. *Fjx1*^{-/-} mice had a germ line mutation, while the *Pkd1* KO was induced in the kidneys of adult mice using the Cre-Lox system. To achieve this, mice of 13 or 14 weeks old were given tamoxifen (5 mg/mouse by oral gavage) for three consecutive days. After one week, mice were given an intraperitoneal injection with DCVC to induce renal injury (15 mg/kg, dissolved in PBS) or PBS as a control.

At several fixed time points after injection, namely 1, 2, 5 and 10 weeks, tissue was obtained. Tissue was also obtained when the blood urea level exceeded 25mmol/l, because this indicated severe kidney failure and therefore the mouse was sacrificed. Renal failure occurred between 11 weeks until 31 weeks after DCVC- or PBS-administration. All groups consisted of 6 mice per time point, which resulted in a total amount of 240 mice for this study. An overview of the experimental groups is given in appendix 2. Of each mouse, 1 kidney was cut transversal and used for histological purposes. All analyses were based on 1 section per mouse.

qPCR

RNA isolation

For RNA isolation, renal tissue was transferred to a MagNa Lyzer tube containing beads. A mix of PBS and 1% 2-Mercaptoethanol (Sigma-Aldrich) was added (500µl) and homogenized for 20 seconds at 7000rpm in the MagNa Lyzer (Roche), followed by another 10 seconds at 7000rpm. The homogenized tissue was dissolved in 1ml Trizol (Ambion), vortexed and incubated at RT for 5 minutes. Subsequently 200µl chloroform (Emsure) was added, samples were shaken for 15 seconds and incubated for 3 minutes at RT. Samples were centrifuged at maximum speed at 4°C for 10 minutes, thereafter the aqueous layer was transferred to a new Eppendorf tube. Consecutively 3µl glycogen (2mg/ml, Roche) and 500µl isopropanol were added, mixed, and incubated for 20 minutes on ice. Samples were centrifuged at maximum speed at 4°C for 10 minutes, the supernatant was discarded and the pellet was washed with 0,5ml ethanol 75% and centrifuged at maximum speed at 4°C for 10 minutes. The ethanol was discarded and the dried pellet was dissolved in 50µl RNase free water (B. Braun). E260/280 was measured using the Nanodrop (ND-1000 spectrophotometer, in combination with the ND-1000 V3.8.1 software).

Generating cDNA

To generate cDNA, 1000ng of RNA was filled up to a total volume of 12,5µl with RNase free water. Samples were incubated for 5 minutes at 65°C, cooled down, centrifuged and kept on ice. A reaction mix was made, containing 4µl 5x RT incubation buffer, 0,5µl oligo-p(dt), 0,4µl AMV-RT (all from Roche), 0,1µl random primers, 2,0µl 10mM dNTP's (both from Invitrogen) and 0,5µl RNasin (Promega). From this mix, 7,5µl was added to the RNA and incubated at 42°C for 60-90 minutes. Samples were incubated for 5 minutes at 85°C and centrifuged.

qPCR

To perform the qPCR, 4,5µl of cDNA (2ng/µl) was added to a 384-wells plate in duplicate. A reaction mix was made of 5µl 2x Faststart Universal SYBR Green Mastermix (ROX) and 0,25µl FW and 0,25µl RV primer (10µM, see table 1 for the sequences). This 5,5µl in total was added to the plate and mixed with the cDNA, whereafter the plate was sealed and centrifuged for 1 minute at 1800rpm.

The qPCR was done in a Roche LightCycler 480, using LightCycler 480 SW 1.5.0.SP3 software. The PCR program was performed in the following steps: 10 minutes at 95°C, 45 cycles of 10 seconds at 95°C, 30 seconds at 60°C and 20 seconds at 72°C, and finally a melting program.

Table 1. Sequence of the used qPCR primers

Primer	Sequence
HPRT FW	GGGTATAAGTTCTTTGCTGACCTG
HPRT RV	AACTTTTATGTCCCCGTTGA
Fjx1 FW	GTGGAGATTGGATCCGAAGA
Fjx1 RV	CTCCCAAAGAGACTGCCATT

Analysis

Results of the qPCR were analysed with the LightCycler 480 SW 1.5.0.SP3 software. T_m was analysed and accepted when there was only one specific peak and the individual sample T_m was close to the average T_m of the primer set. C_t values were determined and accepted when $5 < C_t < 35$ and when the standard deviation of the mean C_t of the duplicates $< 0,2$.

For all accepted samples average C_t of the gene of interest (GOI) and the house keeping gene (HPRT) were calculated. ΔC_t GOI was calculated by subtracting the mean C_t of the housekeeping gene from the C_t of the samples, whereafter the mean of the reference group was determined. Next $\Delta\Delta C_t$ was calculated by ΔC_t GOI – ΔC_t of the reference group. Finally the relative expression ratio was calculated by $RE\ GOI = 2^{(-\Delta\Delta C_t\ GOI)}$ and plotted in a graph. Statistical analysis was done using a 2-way ANOVA (Tukey's multiple comparisons test).

Histology

General

Sections of 4 μm were cut from formalin-fixed paraffin embedded kidneys. After staining, slides were dehydrated, dried, immersed in xylene and coverslipped with mounting medium (CV mount, Leica). Scanning of the slides was done with a Philips ultra-fast scanner 1.6 RA.

PAS staining

PAS staining was performed to measure the cystic index. This was done for the mice at 5 weeks, 10 weeks and failure time point, using 3 sections per group. Exception were the *Fjx1*^{-/-}; *Pkd1* KO and *Pkd1* KO groups at 10 weeks, for those groups all 6 sections were used. After deparaffinization in xylene for 3 times 5 minutes, rehydration in 100% ethanol (twice), 70% ethanol, 50% ethanol and distilled water, sections were oxidized in pre-warmed (48°C) 0,5% periodic acid (Merck) at 48°C for 30 minutes. After washing with aqua dest., sections were stained in Schiff's reagent (Klinipath) for 20 minutes. Next, sections were rinsed for 5 minutes in running tap water, washed with aqua dest. and counterstained in Mayer's haematoxylin for 5 minutes. Finally, sections were rinsed for 5 minutes in running tap water.

Cystic index (CI)

To calculate the cystic index, the scanned PAS-stained sections were saved with a 5x magnification. The photos were opened in Adobe Photoshop CS6, and converted to the Indexed Color mode. The outer edge of the kidney was outflanked and everything except the kidney was deleted. The amount of pixels was read out and noted as pixels 1. If necessary, stained cysts were manually removed, and a color palette was used to remove all color from the cysts. The resulting amount of pixels was read out and noted as pixels 2. Cystic index was calculated according the formula $CI = 100 * ((\text{pixels } 1 -$

pixels 2)/pixels 1). Statistical analysis was done with a Tukey's multiple comparisons test. Only significance for groups with the same treatment (DCVC or PBS) was determined.

Sirius Red staining

Sirius Red staining was performed to measure the Fibrotic Index. For mice from time points 1 and 2 weeks and from renal failure, 3 sections per group were analysed. For time points 5 and 10 weeks, 4 sections were used. After deparaffinization in xylene for 3 times 5 minutes, rehydration in 100% ethanol (twice), 70% ethanol, 50% ethanol and distilled water, sections were predifferentiated in 0,2% phosphomolybdic acid (Applichem) for 5 minutes. Next the sections were stained in 0,1% Sirius Red (0,5g Sirius red (Sigma) in 500ml saturated picric acid (Klinipath)) for 90 minutes in darkness. Differentiation was done for 1 minute in saturated picric acid. Sections were then quickly rinsed in ethanol 70%, and twice in ethanol 100%, immersed in xylene and coverslipped with mounting medium.

Fibrotic Index (FI)

For calculation of the fibrotic index, Sirius red stained sections were used. The scanned sections were saved with a 5x magnification. The photos were opened in Adobe Photoshop CS6, and converted to the Indexed Color mode. A color palette was used to remove all non-stained area. The amount of pixels was read out and noted as pixels 2. After this, a color palette was used to remove all signal except the red color. The resulting amount of pixels was read out and noted as pixels 3. Fibrotic index was calculated according the formula $FI = 100 * (\text{pixels 3}) / (\text{pixels 2})$. All color palettes were checked and (if necessary) adjusted for every batch of stained sections. Statistical analysis was done with a Tukey's multiple comparisons test. Only significance for groups with the same treatment (DCVC or PBS) was determined.

Immunohistochemistry

Lipocalin-2 staining

Damage was visualized by a Lipocalin-2 staining. This was done for all mice who were sacrificed at 24, 48 and 72 hours (2 per group), as well as all mice sacrificed at 1 and 2 weeks (6 per group). After deparaffinization in xylene for 3 times 5 minutes, rehydration in 100% ethanol (twice), 70% ethanol, 50% ethanol and distilled water, heat-induced antigen retrieval (HIER) was performed, using a 10mM Tris/EDTA buffer with pH 9,0^{*}. Sections were incubated for 10 minutes in pre-heated buffer of 100°C and cooled down for at least 20 minutes. After washing with distilled water, endogenous peroxidase was blocked for 20 minutes (0,12% H₂O₂ 30%, Emsure, in distilled water). Sections were washed with distilled water and for 5 minutes with PBS. After incubation with the primary antibody goat- α -mouse LCN-2 (diluted in 1%BSA/PBS 1:150, see table 2 for details) for 1 hour at RT, sections were washed 3 times 5 minutes with PBS. The secondary antibody (rabbit- α -goat Ig/HRP, 1:200, see table 3 for details) was incubated on the sections for 30 minutes, followed by 3 PBS washes for 5 minutes. For visualisation, incubation with DAB⁺ (ratio chromogen:substrate = 1:50, DAKO) was performed for 10 minutes. After washing with distilled water, sections were counterstained in Mayer's haematoxylin for 5 seconds and rinsed in running tap water for 5 minutes. Subsequently, sections were dehydrated and coverslipped with mounting medium. As a positive control, a kidney treated with DCVC and therefore known to contain Lipocalin-2 was used. Two negative controls were used: a

* Tris/EDTA buffer: 12g Tris and 3,7g EDTA diluted in 1l distilled water (=10x stock)

kidney section incubated with normal goat serum instead of the primary antibody and a kidney section known for absence of Lipocalin-2 incubated with the primary antibody.

Lipocalin-2 analysis

To quantify the amount of damage, Lipocalin-2 stained slides of the mice sacrificed at 24, 48 and 72 hours were blindly scored in duplicates on a 3-points scale. Zero represents 0-20% of the tubules diffusely stained, 1 represents 21-50% of the tubules diffusely stained, 2 represents 51-75% of the tubules diffusely stained, while 3 represents >75% of the tubules diffusely stained. Lipocalin-2 stained slides of the 1 and 2 week time points were also blindly scored in duplicates for damage on a 3-points scale, where 0 represents 0-5% of the tubules diffusely stained, 1 represents 6-25% of the tubules diffusely stained, 2 represents 26-50% of the tubules diffusely stained, while 3 represents >50% of the tubules diffusely stained. Scores were averaged and plotted per genotype and treatment. Statistical analysis was done with a Dunn's multiple comparisons test. Only significance for groups with the same treatment (DCVC or PBS) was determined. As a control, the standard deviations of the individual scores for each section of both observers were calculated and the mean of these standard deviations was used to evaluate the inter-observer reliability.

BrdU staining

Proliferation was measured by a BrdU staining. This was done for all mice that were sacrificed at 24, 48 and 72 hours (2 per group). Sections were deparaffinised in xylene for 3 times 5 minutes. After 1 minute in 100% methanol, sections were blocked for endogenous peroxidase in 100% methanol with 0,12% H₂O₂ for 20 minutes. Sections were incubated consecutively in 70% ethanol for 2 minutes, 0,07M NaOH in 70% ethanol for 10 minutes, 70% ethanol for 2 minutes, 70% ethanol for 10 minutes, 50% ethanol for 2 minutes and PBS for 3 times 5 minutes. Sections were incubated for 10 minutes in pre-heated citrate buffer[♦] and cooled down for at least 20 minutes. Next the sections were washed with distilled water, followed by washing with PBS for 2 times 5 minutes. Blocking was done by incubation with 3%BSA/PBST[♠] for 30 minutes at RT. After o/n incubation at 4°C with mouse- α -BrdU, diluted 1:150 in 1%BSA/PBST, sections were washed 3 times 5 minutes with PBST. The secondary antibody (goat α -mouse Envision-HRP) was incubated for 30 minutes, whereafter the sections were washed with PBST for 3 times 5 minutes. For visualisation, incubation with DAB⁺ (ratio chromogen:substrate = 1:50, DAKO) was performed for 10 minutes. After washing with distilled water, sections were counterstained in Mayer's haematoxylin for 5 seconds and rinsed in running tap water for 5 minutes. Subsequently, sections were dehydrated and coverslipped with mounting medium. Tissue without BrdU was used as additional negative control.

BrdU analysis

To calculate the amount of proliferated nuclei, BrdU slides were analysed. BrdU analysis was done with ImageJ (version 1.49). Nine images of the cortex, 5 of the corticomedulla and 1 of the medulla were taken from IMS with a 20x magnification. Pictures were deconvoluted with the "H&E DAB" vector and converted to 8-bit. Threshold was set per slide for the brown and blue colors. Pictures were then run through the commands "despeckle", "fill holes" and "watershed". The parameters for analysing the particles were set at size 100-2000 and circularity 0,4-1, thereby including nuclei of the tubules and excluding nuclei of ECM or a-specifically stained lumen. Mean of the counts of nuclei

[♦] Citrate buffer: 29,41g sodium citrate diluted in 1l distilled water, add citric acid until pH is 6,0 (=10x stock)

[♠] PBST: PBS with 0,1% Tween-20

were calculated for the different kidney areas and tested for significance with a 2-way ANOVA (Sidak's multiple comparisons test).

Table 2. Details primary antibodies

Staining	Primary antibody	Company	Incubation time/temperature	Dilution
Lipocalin-2	Goat- α -mouse LCN-2	R&D systems AF1857	1 hour RT	1:150
BrdU	Mouse- α -BrdU	BD Biosciences (clone B44)	o/n 4°C	1:150

Table 3. Details secondary antibodies

Staining	Secondary antibody	Company	Dilution
Lipocalin-2	Rabbit- α -goat Ig/HRP	DAKO	1:200
BrdU	Goat α -mouse Envision-HRP	DAKO	Ready to use

Cell culture

A murine Inner Medullary Collecting Duct (mIMCD3) cell line (WT) was used to obtain multiple *Fjx1* KO cell lines. Cells were cultured in DMEM/F-12 medium, completed with 10% FCS and 1% penicillin/streptomycin (all Invitrogen) and incubated at 37°C and 5% CO₂. Cell counting was done by mixing a cell suspension with Trypan Blue (1:1), and loading a sample in the Biorad TC10 Automated cell counter. All samples were made in duplicate and measured twice. The mean of the 4 counts was used.

Morphology

Cell lines were compared by eye on morphology characteristics as shape, size and structure. For this purpose, pictures were taken with the BioRevo Eyence BZ-X710 and the related software BZ-X viewer and BZ-X analyser. A 10x magnification and the phase contrast setting were used.

Growth curve

A growth curve was performed to compare the growth rate of the cell lines. Before the actual growth curve was performed, an experiment was done to test the amount of cells which would give a 80% confluence after 5 days of culturing in a 12-wells plate. For this purpose, different numbers of the WT cells were plated in a 12-wells plate and counted after 5 days.

For the growth curve, 3000 cells/well of all cell lines were cultured in triplicate at day 0 in a 12-wells plate with 1,5ml of the medium (described in the second previous paragraph "cell culture"). Every day for the consecutive 5 days, cells were counted and mean and standard deviation were calculated. Results were tested for significance with a 2-way ANOVA (Tukey's multiple comparisons test).

Wound healing

Prior to the wound healing experiment, the cell number needed to get a 100% confluence after 24 hours was determined. This amount of cells was plated in duplicate. After 24h, medium was replaced by serum free medium. Eight hours after this, a scratch was made with a p200 tip,

subsequently cells were washed and normal medium was added. From each well, 2 pictures were taken ($t=0$). After 16 hours ($t=16h$), pictures were taken every two hours at the same location as $t=0$. Analysis was done using ImageJ. In every picture, at least 20 lines between the edges of the scratch were drawn with ImageJ, and the mean of their length was taken. The mean of the 4 replicates per cell type was plotted as percentage of the original wound and compared for all time points and cell types using a 2-way ANOVA (Tukey's multiple comparisons test).

Results

***Fjx1* expression is increased in WT mice compared to *Pkd1* KO mice at the 10 week time point**

Happé (2009) found that expression of *Fjx1* first showed a decrease and later an increase in the *PKD1* KO mice, while in the WT mice expression of *Fjx1* first showed an increase and afterwards a decrease. This experiment was repeated in the current study. First a qPCR with an input of 2,5µl of cDNA was done. Standard deviations of the Ct duplicates with *Fjx1* primers and *HPRT* were rather high (mean SD = 0,26 for *Fjx1* samples and 0,15 for *HPRT* samples with peaks for certain samples near 1 Ct, while a SD of 0,2 is considered as acceptable). This indicates a low reliability of the experiment. The qPCR was repeated by my supervisor with an input of 4,5µl cDNA, still resulting in high standard deviations for *Fjx1* samples (mean SD = 0,25). Results of the second experiment showed increased mRNA expression of *Fjx1* in WT mice compared to *Pkd1* KO mice, although this difference was only significant for the 10 week time point. *Fjx1* expression was increased at later time points in *PKD1* KO mice and in WT first an increase and afterwards a decrease was seen, shown in figure 4.

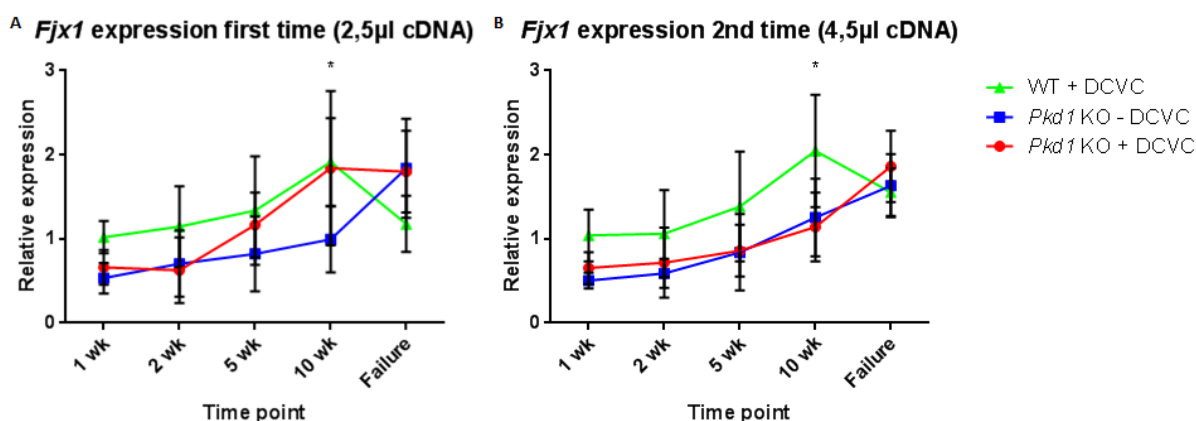


Figure 4. mRNA expression of *Fjx1*, normalized to the mean expression of the WT 1 week samples. Data was displayed as mean \pm SD of the 6 mice per group. Statistical analysis was done with a Tukey's multiple comparisons test. In A: * = significant difference *Pkd1* - DCVC compared to *Pkd1* KO + DCVC ($p \leq 0,05$) and WT compared to *Pkd1* KO - DCVC ($p \leq 0,01$) In B: * = significant difference WT compared to *Pkd1* KO + DCVC ($p \leq 0,001$) and WT compared to *Pkd1* KO - DCVC ($p \leq 0,01$)

***Pkd1* KO and *Fjx1*^{-/-}; *Pkd1* KO mice show an increased cystic index at 10 weeks and failure time points**

The amount of cysts contributes to the onset of renal failure. To investigate the difference in age at renal failure for the *Fjx1*^{-/-}; *Pkd1* KO and *Pkd1* KO mice, the amount of cysts was determined on PAS-stained slides at 5 and 10 weeks, as well as renal failure. Observations showed a difference between the models, as can be seen in figure 5. At failure, the DCVC-treated *Fjx1*^{-/-}; *Pkd1* KO and *Pkd1* KO mice showed cyst formation while this was absent in the *Fjx1*^{-/-} and WT mice. This difference also translated in differences in cystic index (CI) between the groups, shown in figure 6. For the 5 week time point, no differences in CI were seen between the genotypes. At 10 weeks, the DCVC-treated *Fjx1*^{-/-}; *Pkd1* KO and *Pkd1* KO mice showed a significant higher CI compared to the *Fjx1*^{-/-} and WT mice (significant at $p \leq 0,01$ and $p \leq 0,05$ respectively). For the failure time point, the same significant

differences were seen for both the DCVC- and PBS treated animals (significant at $p \leq 0,0001$ and $p \leq 0,001$ respectively for the DCVC-treated mice and significant at $p \leq 0,0001$ for the PBS-treated mice). The DCVC-treated *Fjx1*^{-/-};*Pkd1* KO and *Pkd1* KO mice did not differ significantly from each other. Although differences in the amount of cysts between DCVC- and PBS-treated mice were visible by eye, the CI of these mice resulted in only small differences.

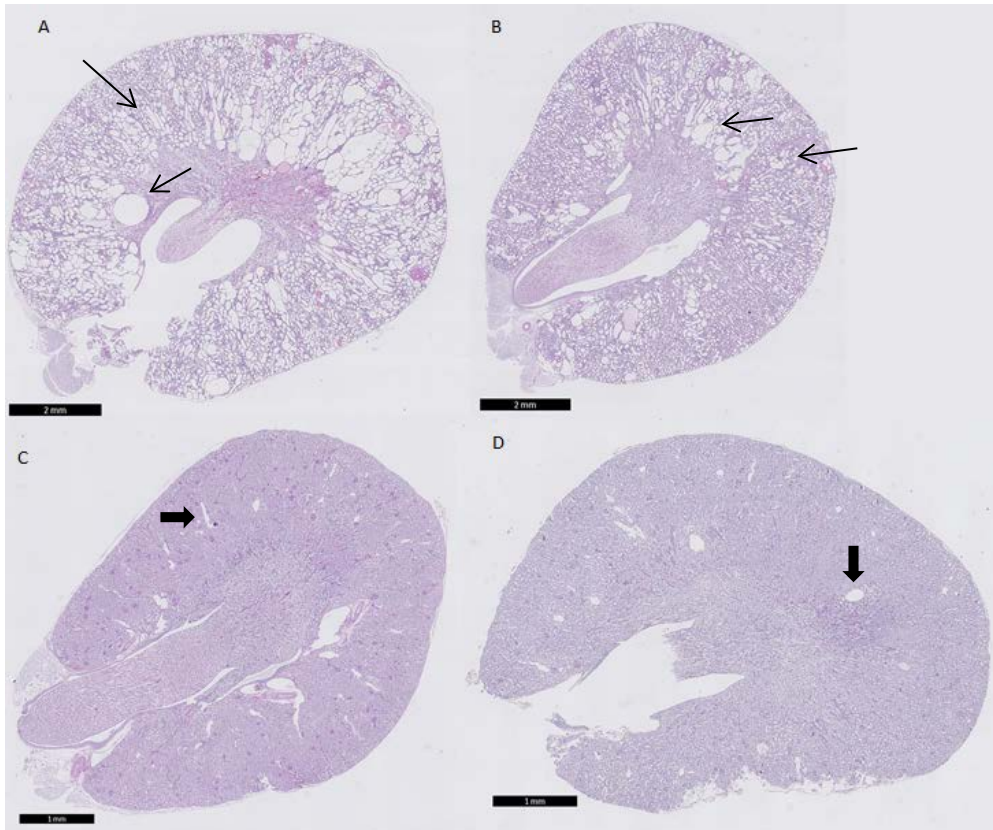


Figure 5. Representative PAS stained sections of a kidney from the renal failure time point of (A) a *Fjx1*^{-/-};*Pkd1* KO mouse, (B) a *Pkd1* KO mouse, (C) a *Fjx1*^{-/-} mouse and (D) a WT mouse. Arrows: cysts, broad arrows: blood vessels.

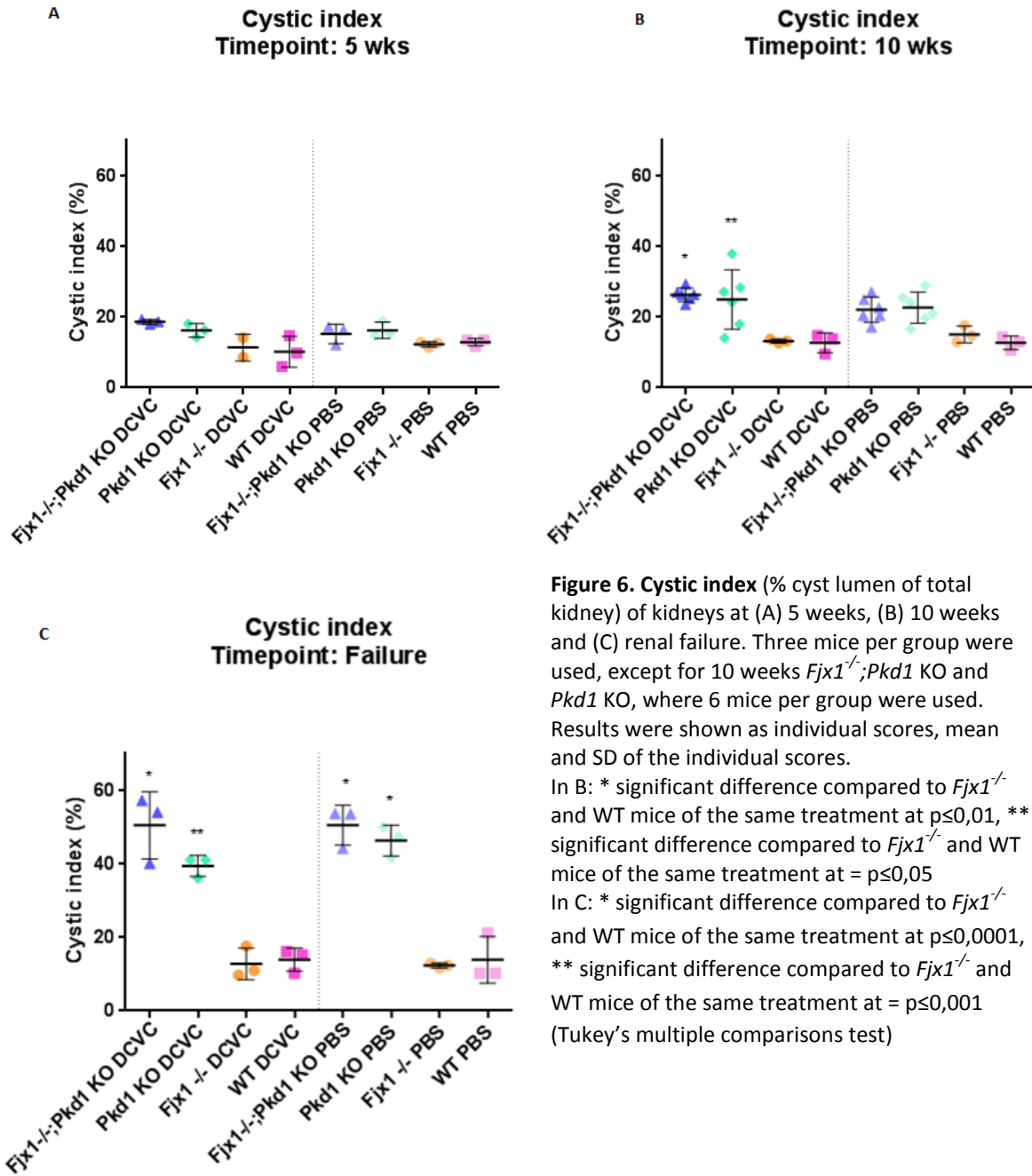


Figure 6. Cystic index (% cyst lumen of total kidney) of kidneys at (A) 5 weeks, (B) 10 weeks and (C) renal failure. Three mice per group were used, except for 10 weeks *Fjx1*^{-/-};*Pkd1* KO and *Pkd1* KO, where 6 mice per group were used. Results were shown as individual scores, mean and SD of the individual scores. In B: * significant difference compared to *Fjx1*^{-/-} and WT mice of the same treatment at $p \leq 0,01$, ** significant difference compared to *Fjx1*^{-/-} and WT mice of the same treatment at $p \leq 0,05$. In C: * significant difference compared to *Fjx1*^{-/-} and WT mice of the same treatment at $p \leq 0,0001$, ** significant difference compared to *Fjx1*^{-/-} and WT mice of the same treatment at $p \leq 0,001$ (Tukey's multiple comparisons test)

***Fjx1*^{-/-};*Pkd1* KO mice show slightly less damage compared to *Pkd1* KO mice**

To visualize the amount of cellular damage in the kidney, a Lipocalin-2 staining was performed on kidneys from the 24, 48 and 72 hour time points, as well as 1 and 2 week time points. Staining showed two kinds of Lipocalin-2 deposition patterns. Firstly a cytoplasmic diffuse staining in tubules was seen and secondly, a cytoplasmic pattern of dots at the apical side of the nucleus was observed, see also figure 7. The cytoplasmic diffuse staining is the one described in literature as a result of the damage¹⁸ and therefore scored, using a 3-points scale. The negative control showed no staining, and the sections from PBS-treated mice showed a largely reduced amount of staining.

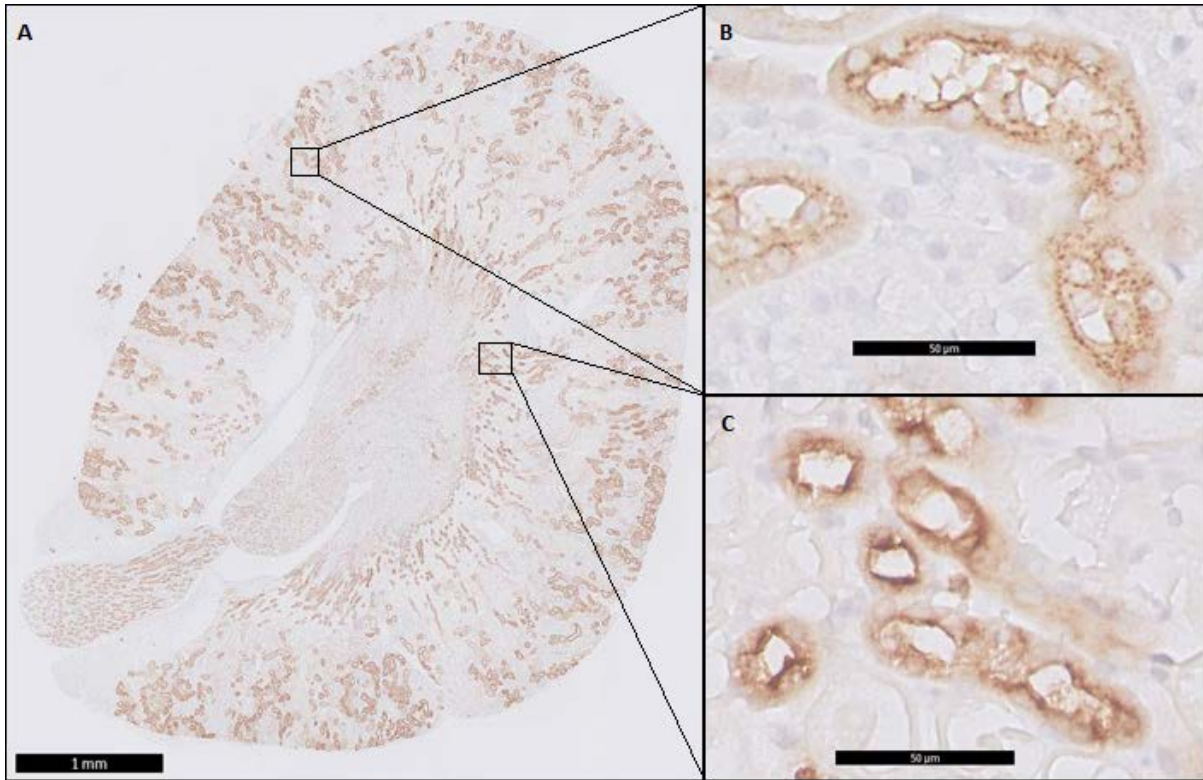
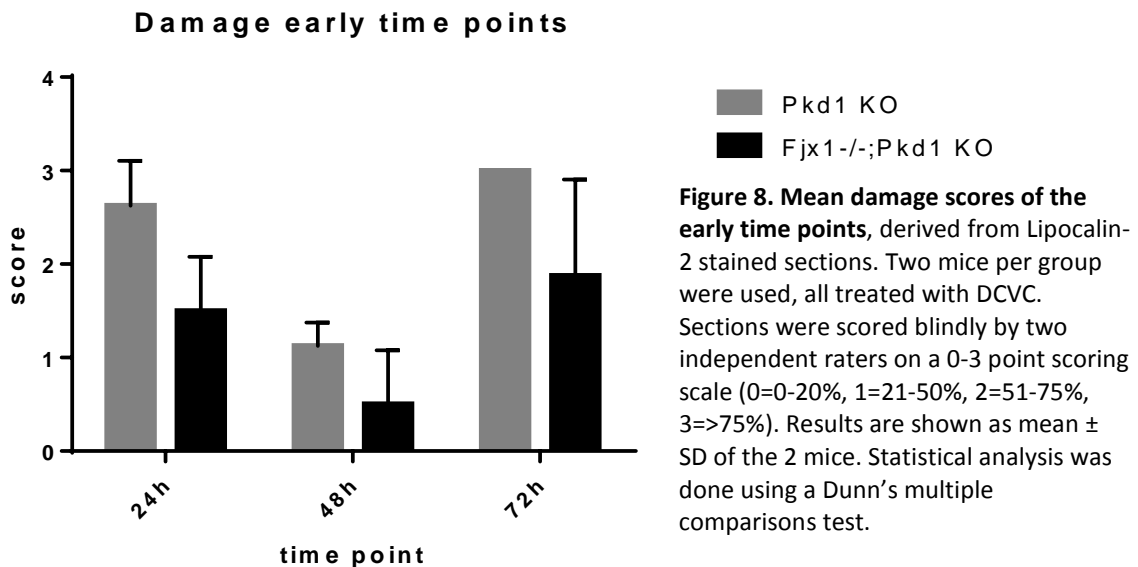


Figure 7. Representative Lipocalin-2-stained slide of a *Pkd1* KO mouse sacrificed at 24 hours. (A) overview of the whole kidney, (B) pattern of dots, (C) diffuse cytoplasmic staining.

For the early time points (the pilot) the *Fjx1^{-/-};Pkd1* KO mice seemed to show a lower damage score compared to the *Pkd1* KO mice (see figure 8), but this was not significantly different. Mean of the inter-observer standard deviation was 0,08, which indicates a high inter-observer reliability.



The DCVC-treated mice showed a trend in reduction of the damage in time at 1 and 2 weeks, but this was not significant. No differences were seen between the genotypes of the same time point, although a big variation within the groups was observed. Just as in the early time points, the *Fjx1^{-/-};Pkd1* KO mice tended to have a lower damage score compared to the *Pkd1* KO mice. Mean of the inter-observer standard deviation was 0,15 for the 1 week time point and 0,09 for the 2 week time

point, which indicates a reasonably high to high inter-observer reliability. Results are shown in figure 9.

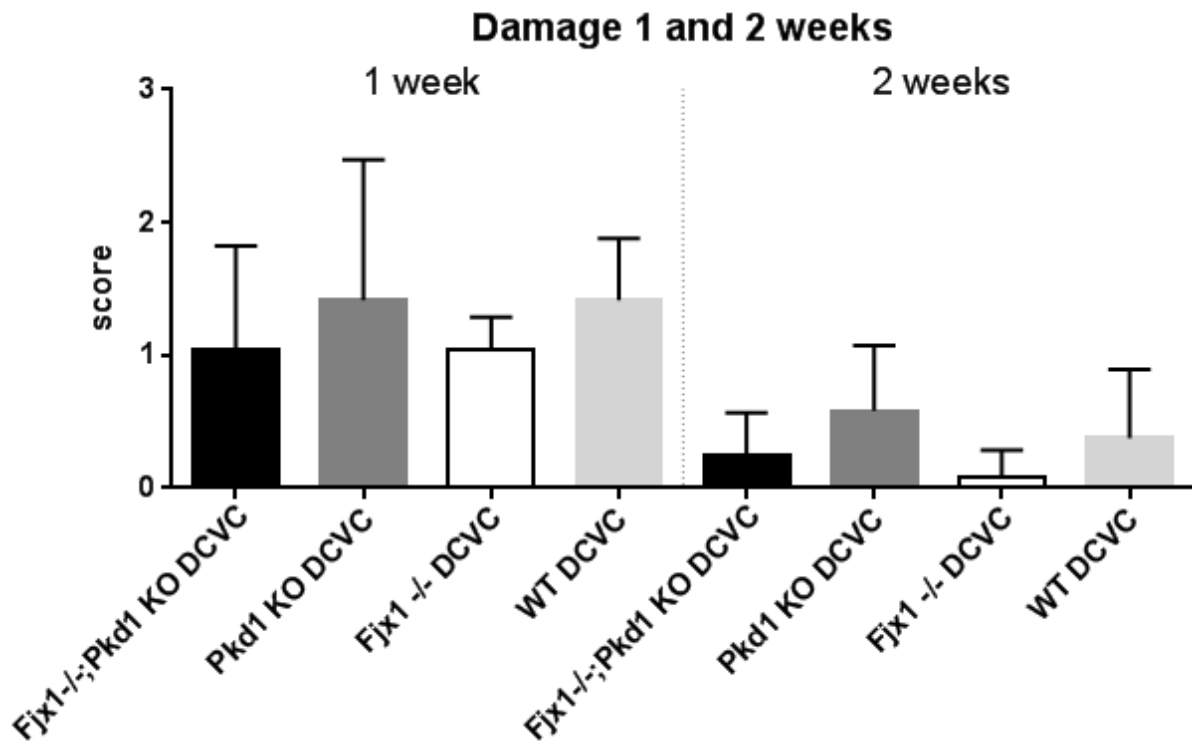


Figure 9. Mean damage scores of the 1 and 2 week time points for the DCVC-treated mice, derived from Lipocalin-2 stained sections. Six mice per group were used, all treated with DCVC. Scores were scored blindly by two independent raters on a 0-3 point scoring scale (0=0-5%, 1=6-25%, 2=26-50%, 3>50%). Results are shown as mean \pm SD of the 6 mice. Statistical analysis was done using a Dunn's multiple comparisons test.

Early time points *Fjx1*^{-/-}; *Pkd1* KO mice show no difference in proliferation compared to *Pkd1* KO mice

During repair, various processes can be distinguished. Two of them are proliferation and fibrogenesis. Markers for both of them were used to gain information about repair in the mouse models. For the early time points, slides were stained for BrdU to demonstrate the amount of proliferation. The percentage of BrdU-positive nuclei in the cortico-medullary region is shown in figure 10, showing equal amounts of proliferated nuclei for both genotypes. The negative control showed no staining, as well as the control without BrdU (a 1 week WT mouse). Results were not significantly different. The percentage increased as time passes after DCVC-administration, also seen in the slides shown in figure 11.

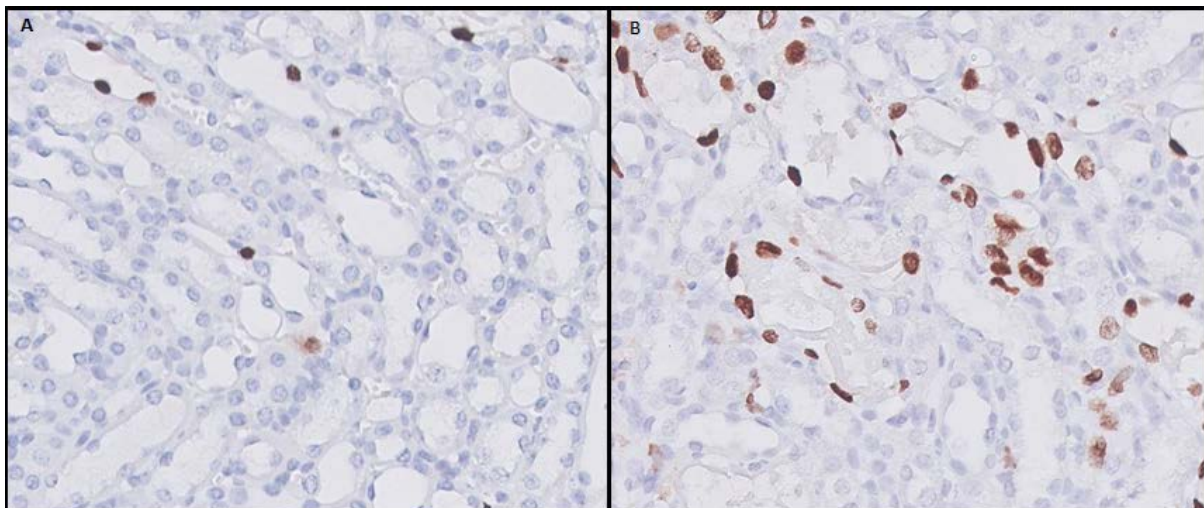
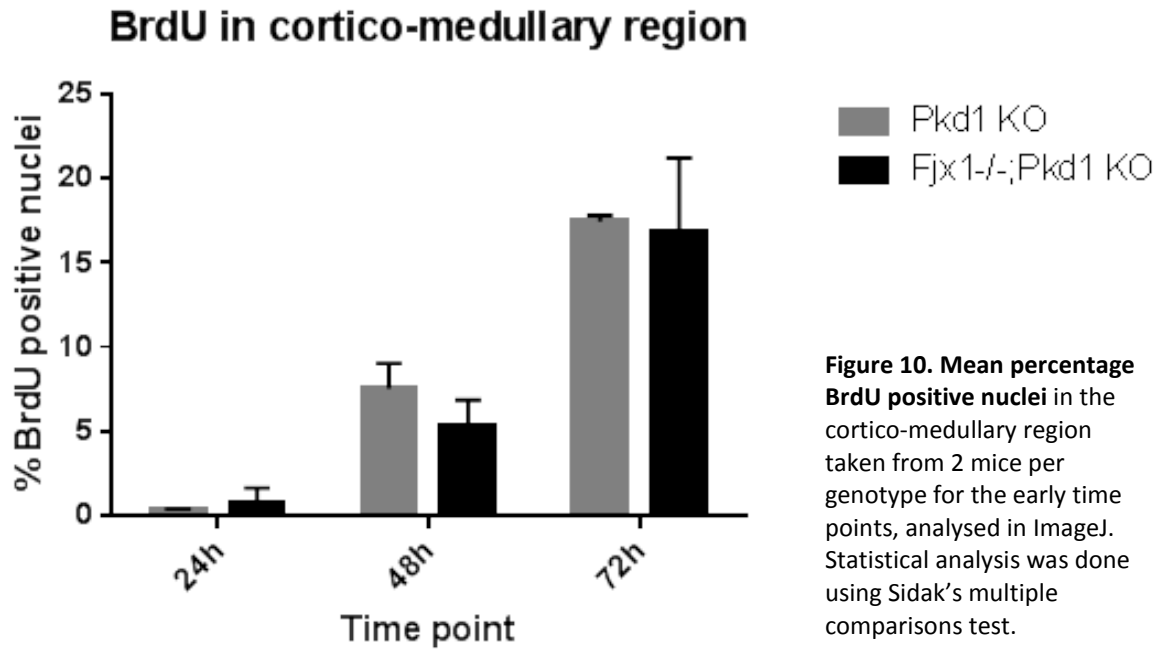
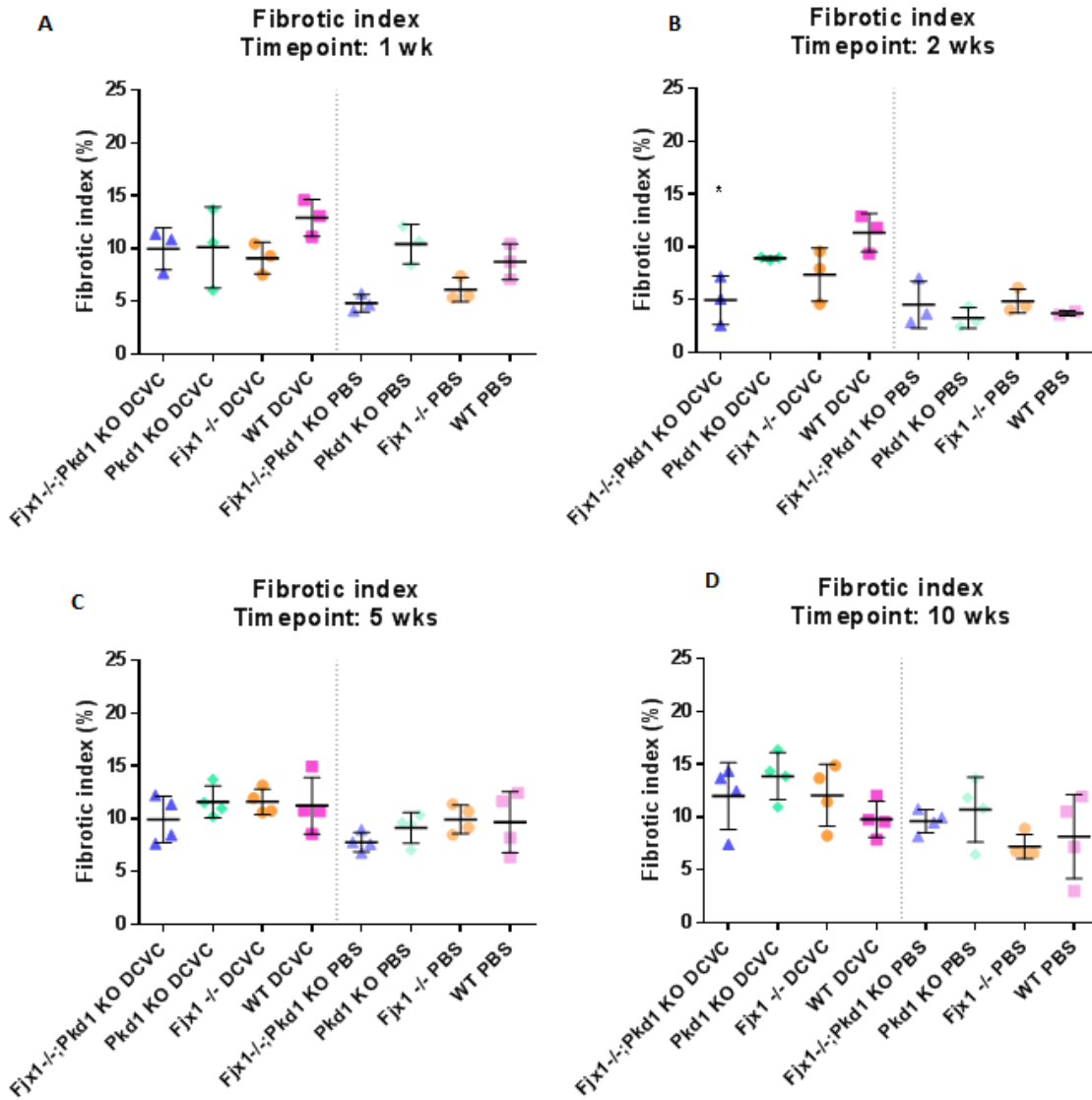


Figure 11. Representative 200x photos of the cortico-medullary region of BrdU-stained slides of a *Fjx1^{-/-};Pkd1* KO mouse at (A) 24 hours and (B) at 72 hours.

***Fjx1^{-/-};Pkd1* KO mice show no relevant differences in fibrotic index compared to *Pkd1* KO mice**

Fibrosis was demonstrated in kidneys at 1, 2, 5 and 10 weeks and at renal failure with the fibrotic index (FI), derived from the Sirius Red stained slides. All slides showed fibrosis in the medulla, which extended to the cortico-medullary region area when the amount of fibrosis increased. The slides with a high amount of cysts also showed fibrosis in the cortex. Results of the FI are shown in figure 12. At 1 week there was a slightly higher FI for the WT DCVC mice compared to the other DCVC-treated models. The PBS-treated *Fjx1^{-/-};Pkd1* KO and *Fjx1^{-/-}* mice showed a lower FI compared to the other PBS-treated animals, although differences were not significant. Mice at 2 weeks showed a higher FI for the *Pkd1* KO- and the WT DCVC-treated mice, compared to the *Fjx1^{-/-};Pkd1* KO and *Fjx1^{-/-}*

^{-/-} DCVC-treated mice. This difference between the *Fjx1*^{-/-}; *Pkd1* KO- and WT DCVC-treated mice was significant. At 5 weeks, no differences were seen between the different phenotypes. The same applied for the 10 week time point, although the *Pkd1* KO model had a slightly higher FI. At renal failure, the *Fjx1*^{-/-}; *Pkd1* KO and the *Pkd1* KO mice in both the DCVC- and PBS-treated groups showed a higher FI compared to the *Fjx1*^{-/-} and WT mice, although only the difference between the PBS-treated *Pkd1* KO mice and the *Fjx1*^{-/-} mice was significant.



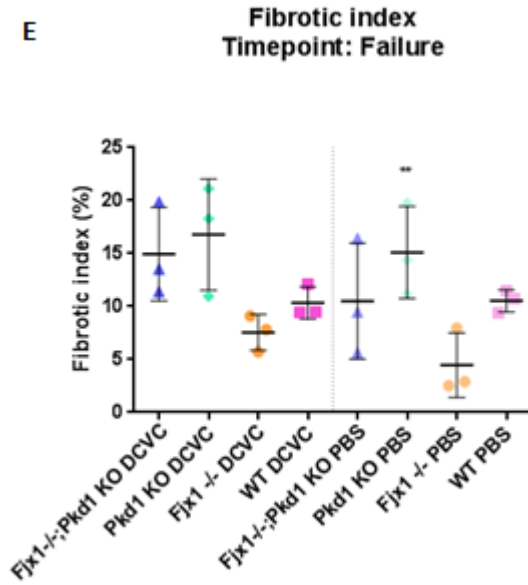


Figure 12. Fibrotic index (% fibrosis of total tissue) of kidneys at (A) 1 week, (B) 2 weeks, (C) 5 weeks, (D) 10 weeks and (E) renal failure. Three mice per group were used, except for 5 and 10 week time points, where 4 mice per group were used. Results were shown as individual scores, mean and SD of the individual scores. . At 2 weeks, DCVC-treated *Fjx1*^{-/-}; *Pkd1* KO mice showed a significantly lower FI compared to the DCVC-treated WT mice (*, $p \leq 0,01$). At failure, PBS-treated *Pkd1* KO mice showed a significantly higher FI compared to PBS-treated *Fjx1*^{-/-} mice (**, $p \leq 0,05$) (Tukey's multiple comparisons test).

Characterization of *Fjx1* KO cell lines

Fjx1 KO cells appear to have the same morphology compared to WT cells

To be able to study the influence of the *Fjx1* gene *in vitro*, two separate knock out cell lines for *Fjx1* were generated, named P2 and P5. The newly generated cell lines were compared to each other and to the WT cell line for their morphology. This was done by looking at the shape of the cells, the size and the structure. Cell lines are shown in figure 13. All cell lines showed an epithelial-like shape (polygonal). Also all cell lines had clearly visible nucleoli. Cells of P2 seemed to be larger because more cytoplasm was seen. This was probably due to small differences in confluence.

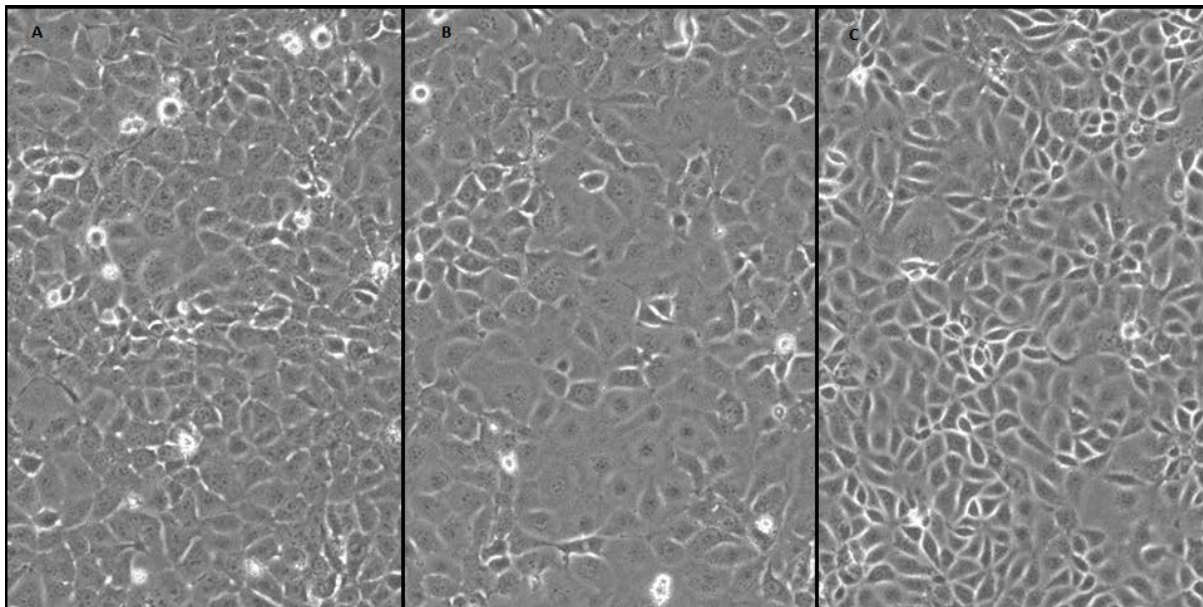


Figure 13. Morphology. Representative 100x photos of (A) the WT cells, (B) P2 and (C) P5.

WT cells have a higher growth rate compared to *Fjx1* KO cells

WT and *Fjx1* KO cell lines were also compared for growth rate. An equal amount of plated cells was counted for 5 consecutive days after plating. The WT cell line showed a significantly higher growth rate at day 4 and 5 compared to the *Fjx1* KO (P2 and P5) cell lines. Results are shown in figure 14. Repetition of this experiment confirmed the findings and also showed a significantly higher growth rate for P2 compared to P5 at day 4 and 5, respectively at $p \leq 0.01$ and $p \leq 0.0001$.

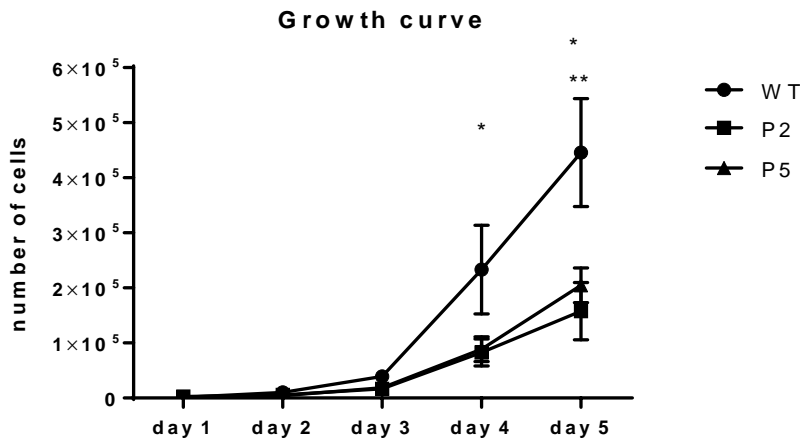


Figure 14. Growth curve of WT and *Fjx1* KO cell lines. At day 0, 3000 cells were plated in triplicate for each cell line, and counted on 5 consecutive days. Results were shown as mean of the triplicates \pm SD. Statistical analysis was done using a Tukey's multiple comparisons test. * = significant difference WT compared to P2 and P5 at $p \leq 0.0001$, ** = significant difference P2 compared to P5 at $p \leq 0,05$

Wound healing

Because of the suspected role of *Fjx1* in the repair mechanism, the *Fjx1* KO cell lines were compared to the WT for their ability to recover after injury. This was done using a wound healing assay. In figure 15, (A) shows the WT cell line after the scratch was made. (B), (C) and (D) show the amount of closure at respectively $t=16h$, $t=20h$ and $t=24h$. Overall results are shown in figure 16, revealing the fastest closure for P5, followed by the WT cells and P2 showing the slowest closure. This was significantly different for P2 versus P5 and the WT cell line at $t=16h$, $t=18h$ and $t=20h$. Estimated confluence at the starting point was for P5 100%, for the WT 95% and for P2 85%.

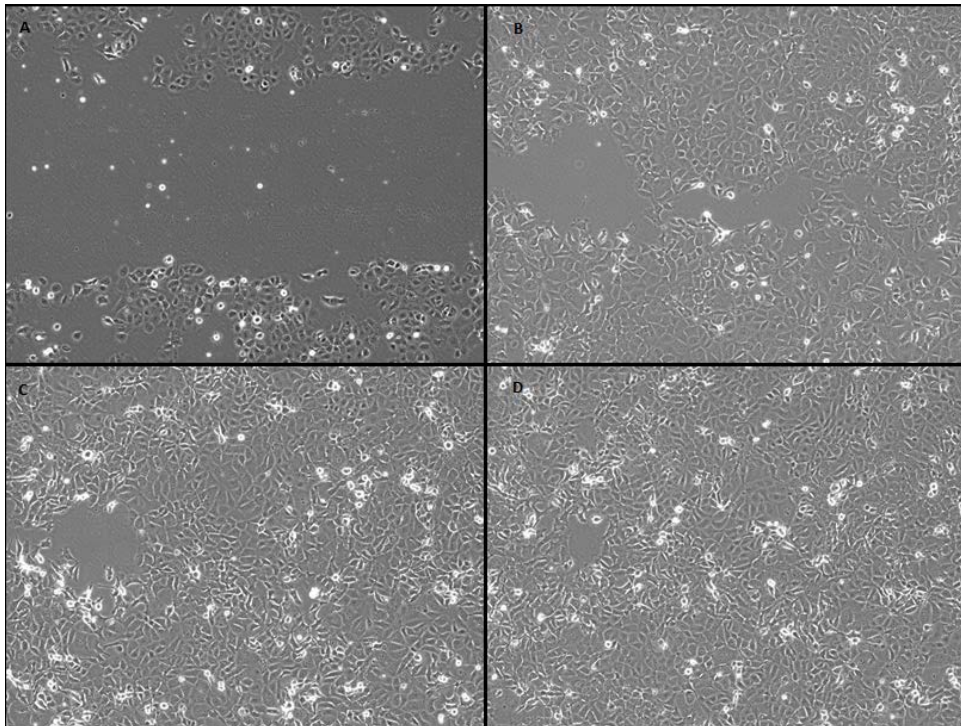


Figure 15. Wound healing. Representative 100x photos of the WT cells at (A) t=0, (B) t=16h, (C) t=20h and (D) t=24h, showing the closure of the wound in time.

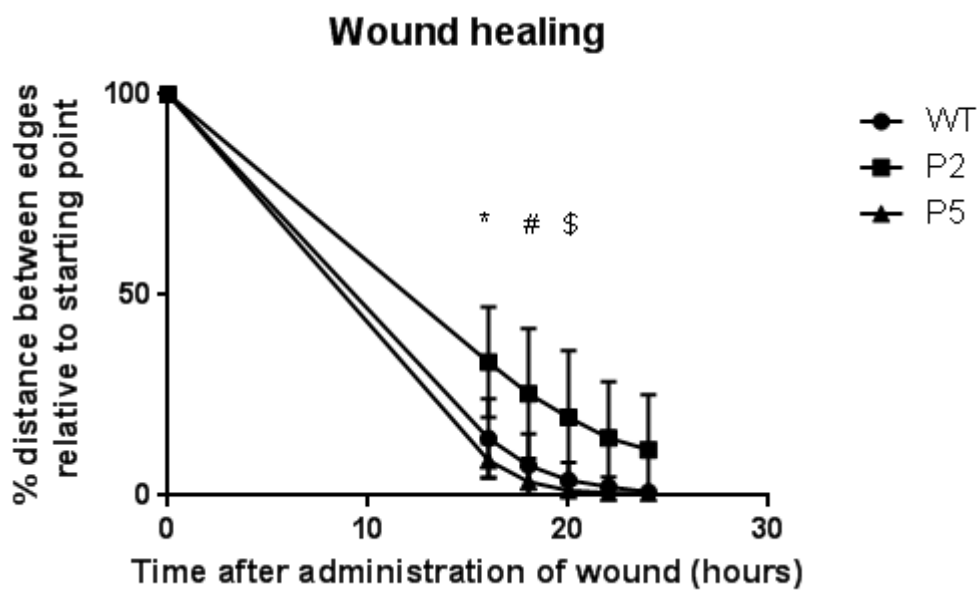


Figure 16. Wound healing assay for WT and *Fjx1* KO cell lines. At t=0, a scratch was made in 100% confluent cells, seeded in duplicate. Of each scratch, 2 pictures were taken at t=0, t=16 and every 2 hours thereafter until the wound was fully closed. Distances of the wound edges were calculated in ImageJ and normalized relative to t=0. Statistical analysis was done using a Tukey's multiple comparisons test. * significant difference between P2 and WT ($p \leq 0,01$) and between P2 and P5 ($p \leq 0,001$); # significant difference between P2 and WT ($p \leq 0,05$) and P2 and P5 ($p \leq 0,01$); \$ significant difference between P2 and WT and P2 and P5 ($p \leq 0,05$).

Discussion and conclusion

This study examined the role of *Fjx1* in the context of ADPKD, especially to gain more insight into the mechanism which causes a later onset of renal failure after induction of injury in a *Fjx1*^{-/-};*Pkd1* KO model compared to a *Pkd1* KO model.

To do so, this study focused on the characterization of some of the principal mechanisms involved in injury and repair, namely: tissue damage, cell proliferation and fibrosis. Also the amount of cysts, a hallmark of ADPKD, was investigated.

Preliminary data of Happé (2009) showed an increased mRNA expression of *Fjx1* in WT mice after administration of DCVC, while the *Pkd1* KO mice exhibited a decreased mRNA expression after DCVC-administration. This opposite expression was the motivation for this study. We therefore verified mRNA expression of *Fjx1* in our mouse models, which was determined using a qPCR. The high standard deviation between the raw Ct values of the first experiment (using 2,5µl cDNA), indicated a low reliability and further analysis of the Ct's revealed high Ct values (around 31). This indicated a low amount of mRNA, favouring a high standard deviation. In the second performance, using 4,5µl cDNA, still a high standard deviation between the raw Ct values was seen. When this experiment is going to be repeated, a (much) higher concentration of cDNA (for example 15ng/µl instead of 2 ng/µl) will be required. Other differences regarding both performances seem to be due to differences of precise pipetting, but also a possibility of (protein)dilution in the mRNA which interferes with the reaction cannot be excluded.

Due to this technical problem we were not able to replicate the original data shown in the experiment of Happé (2009). Nevertheless the role of *Fjx1* in the injury/repair process emerged also from preliminary data obtained in this study, therefore the hypothesis of a role for *Fjx1* in injury/repair still stands.

The amount of cysts contributes to the onset of renal failure. To investigate a possible difference in cyst formation for the DCVC-treated *Fjx1*^{-/-};*Pkd1* KO and *Pkd1* KO mice, the amount of cysts was determined on PAS-stained slides at 5 and 10 weeks, as well as renal failure. Both *Pkd1* KO mouse models developed cysts later in life, in contrast to the *Fjx1*^{-/-} and WT mice which never developed cysts. Because a mutation of the *Pkd1* gene is known to be a major contributor in the pathogenesis of ADPKD, this was as expected. For the *Fjx1*^{-/-};*Pkd1* KO and *Pkd1* KO mice of 5 and 10 weeks and renal failure, no difference has been found, indicating a similar degree of cyst formation. This suggests that the amount of cyst formation does not contribute to the later onset of renal failure in DCVC-treated *Fjx1*^{-/-};*Pkd1* KO mice compared to *Pkd1* KO mice.

Surprisingly the difference in CI between DCVC- and PBS-treated mice was very small, despite clear differences in cyst formation visible by eye. This indicates a medium sensitivity of the analysis method, which could be increased by using a higher magnification for the photos.

Damage was visualized by immunohistochemistry using an antibody against Lipocalin-2. The Lipocalin-2 staining showed multiple patterns of staining; firstly a cytoplasmic diffuse staining in tubules was seen, caused by the damage induced by DCVC; secondly, a cytoplasmic pattern of dots at the apical side of the nucleus could be seen. This is suspected to be caused by reabsorption of the excreted Lipocalin-2 by the proximal tubules.¹⁸ These distinct staining patterns complicated the scoring of the damage. Scoring was done by eye by two independent raters. At first a scale system was used, comparing slides between themselves with slides of the WT as a reference. This resulted in a slightly intermediate inter-observer reliability (mean SD = 0,3 for the 1 week time point). When

switched to a rating system for percentage of area stained, a higher inter-observer reliability was achieved (mean SD = 0,15 for the 1 week time point), indicating a higher reliability of the scores itself. Although a distinction was made between both staining patterns, it could have influenced the scores. For this reason it is advised to examine also different markers for damage in future investigations. A suitable marker requires to be increased specifically by any damage and must show an univocal staining pattern. A possible candidate could be heme oxygenase 1 (HO-1), an enzyme involved in breakdown of heme which is increased after oxidative stress.²¹

The staining of Lipocalin-2 for the early time points (sacrificed at 24, 48 and 72 hours after DCVC) seemed to show less depositions in the *Fjx1*^{-/-};*Pkd1* KO kidneys compared to the *Pkd1* KO kidneys, which indicated less damage in the kidneys of the *Fjx1*^{-/-};*Pkd1* KO mice. Although this difference was not significant, it showed a trend suggesting absence of *Fjx1* could be protective against damage.

This experiment was done in a small group of 2 mice per genotype, therefore using bigger groups of 6 mice would produce a more stronger, definitive result. Before setting up the experiment, it was calculated that 6 mice per group would give enough power to yield reliable results.

For mice at 1 and 2 weeks, the same general trend was seen, i.e. both *Fjx1* KO genotypes tended to have less Lipocalin-2 in the kidney compared to the *Pkd1* KO and WT mice, supporting a hypothesis of a lower sensitivity to the damage. However, a lot of variation was seen within the groups, therefore tissue of all six mice per group was examined. This didn't result in a more evident result. This could be due to the fact that the damaged renal tissue of the mice of the 1 and 2 weeks time points were already in an advanced repair phase, which could cause differences in amount of stained damage per individual mice. Indeed when comparing the scores of the kidney at 1 and 2 weeks per genotype, a reduction of positive Lipocalin-2 staining was seen, indicating repair. This is also consistent with previous findings of Happé (2009), where damage was repaired within a time period of approximately two weeks. Further research could focus on damage arising from cyst formation at later time points, perhaps helping to clarify the difference found in age of renal failure.

Proliferation for the early time points was quantified through an immunohistochemical BrdU-staining. It was hypothesized that a faster repair of the damage could lead to the found delay of renal failure in the *Fjx1*^{-/-};*Pkd1* KO model compared to the *Pkd1* KO model (treated with DCVC). Characterization of the proliferation could lead to acceptance or rejection of this hypothesis. Results showed similar amounts of proliferation for both genotypes, suggesting that the rate of repair in the *Fjx1*^{-/-};*Pkd1* KO model was not different from the one observed in the *Pkd1* KO model. Therefore this cannot explain the differences observed in survival among the two genotypes. Nevertheless it is important to keep in mind that this was a pilot experiment conducted on only two mice per group, therefore results cannot be definitive but can only be used as an indication of the real mechanism which needs to be further studied, eventually by using bigger groups of 6 mice.

Fibrosis is a well-known product of the damage repair process and is also a cause of kidney failure.²² A difference in fibrosis could therefore explain the observed difference in survival among the genotypes. For the later time points the amount of fibrosis was quantified using a Sirius Red staining. This staining is known to be sensitive to differences in color intensity among different sessions of staining, making it necessary to adjust the Photoshop palette used for analysis for every stained batch. As a consequence, it was only possible to make comparisons among the same stained batch of tissue. In this study, sections were stained per time point, because a comparison between genotypes was preferred. To check whether the staining was really catching differences in amount of

fibrosis instead of differences in staining (due to differences in color intensity between different stained batches), a few slides of every time points were stained at the same time as control. Analyses from Photoshop were also checked by comparing the amount of fibrosis measured with the software and the amount of fibrosis observed by eye. The amount of fibrosis was similar for the different genotypes. This suggests that the amount of fibrosis is not the cause of the found difference in age at renal failure. Despite this result, all genotypes expressed a low amount of fibrosis in general. Differences between DCVC-treated mice and PBS-treated mice were also small, although we expected to see a more clear difference between those groups. Therefore it cannot be excluded that the lack of differences may be due to the fact that the analysis is not sensitive enough to pick up the small differences. For this reason, the mRNA of several fibrosis-associated genes like collagen1a1, vimentin, TGF- β 1, α -SMA and fibronectin will be quantified. Acquiring the pictures used in analysis with a higher magnification would also yield more details and therefore would pick up small differences.

Aside from the *in vivo* experiments, to gain more insight in the role of *Fjx1*, also *in vitro* experiments were performed. A reduced growth rate of *Fjx1* KO cells compared to a WT cell line was observed, though it is not yet clear how this can be related to a lower sensitivity to the damage observed in our mouse models. One of the two cell lines (*Fjx1* KO P5) showed a particular lower growth rate, both in a growth curve assay as in normal culture condition, suggesting an off-target effect of the technique used to achieve the KO. This underlines the importance of using more than one cell line clone to sort out the real phenotype from eventual clone-bias. Repetition of the growth curve experiment confirmed the higher growth rate of the WT cell line, but also showed a higher growth rate for the *Fjx1* P2 cell line compared to the first experiment, although still significantly lower than the WT cell line. This indicates that a better control of the experiment variables is needed in order to have reproducible and reliable results. This could be achieved by using a higher amount of cells, what is to be tested in a six-wells plate.

To gain insights in cell migration processes and cell-cell interaction processes, a wound healing assay was performed. Reliability of this experiment is questionable due to differences in confluence at the starting point. Despite of testing the amount of cells needed in advance, still differences in confluence occurred at the very moment of the experiment. When repeated, an equal confluence of all cell lines when creating the wound is important. It would also be interesting to measure more early time points (for example 4, 8 and 12 hours) to gain more information on the onset of the cell migration process.

Preliminary experiments showed a difference in onset of renal failure between the *Fjx1*^{-/-};*Pkd1* KO and *Pkd1* KO mice. In *Pkd1* KO mice, a faster development of the disease in DCVC-treated animals compared to PBS-treated animals was observed, while the *Fjx1*^{-/-};*Pkd1* KO mice did not show this difference. Indeed both DCVC- and PBS-treated animals in the latter genotype got renal failure at approximately the same age.

In these experiments, it was demonstrated that this difference was not due to differences in amount of cyst formation, proliferation or fibrosis, although there seems to be indeed a tendency for reduced damage in absence of *Fjx1*. This means that the mechanism through which the lack of *Fjx1* is protective against damage in renal epithelial cells in ADPKD mouse models is still unclear. Further research is needed to unveil the causative mechanism, also focusing on the late time points, i.e. the 10 weeks and renal failure. At these time points, severe damage occurs due to the formation of

cysts, while renal failure is delayed in the *Fjx1*^{-/-};*Pkd1* KO DCVC-treated mice model compared to the *Pkd1* KO DCVC-treated mice. These differences deserve further investigation.

References

1. Neumann HPH, Jilg C, Bacher J, Nabulsi Z, et al. "Epidemiology of autosomal-dominant polycystic kidney disease: an in-depth clinical study for south-western Germany". *Nephrol Dial Transplant*. **2013**; Vol.28: p1472-87
2. Akoh JA. "Current management of autosomal dominant polycystic kidney disease". *World J Nephrol* **2015**; Vol.4: p468-479
3. Happé H, Peters DJM. "Translational research in ADPKD: lessons from animal models". *Nat. Rev. Nephrol*. **2014**; Vol.10: p587-601
4. Blair HA, Keating GM. "Tolvaptan: A Review in Autosomal Dominant Polycystic Kidney Disease". *Drugs*. **2015**; Vol.75: p1797-806
5. Chapin HC, Caplan MJ. "The cell biology of polycystic kidney disease". *J Cell Biol*. **2010**; Vol.191: p701-710
6. Bastos AP, Onuchic LF. "Molecular and cellular pathogenesis of autosomal dominant polycystic disease". *Braz J Med Biol Res* **2011**; Vol.44: p606-617
7. Happé H, Van der Wal AM, Leonhard WN, Kunnen SJ, et al. "Altered Hippo signalling in polycystic kidney disease". *J Pathol*. **2011**; Vol. 224: p133-142
8. Sebbagh M, Borg JP. "Insight into planar cell polarity". *Exp Cell Res*. **2014**; Vol.328: p284-95
9. Tepass U, Truong K, Godt D, Ikura M, et al. "Cadherins in embryonic and neural morphogenesis". *Nat Rev Mol Cell Biol*. **2000**; Vol.2: p91-100
10. Jolly MK, Rizvi MS, Kumar A, Sinha P. "Mathematical Modeling of Sub-Cellular Asymmetry of Fat-Dachsous Heterodimer for Generation of Planar Cell Polarity". *PLoS One* **2014**; Vol.9: e97641
11. Happé H, Leonhard WN, Van der Wal A, Van de Water B, et al. "Toxic tubular injury in kidneys from Pkd1-deletion mice accelerates cystogenesis accompanied by dysregulated planar cell polarity and canonical Wnt signaling pathways". *Hum Mol Genet*. **2009**; Vol.18: p2532-42
12. Hale R, Strutt D. "Conservation of Planar Polarity Pathway Function Across the Animal Kingdom". *Annu. Rev. Genet*. **2015**; Vol.49: p1.1-1.23
13. Grusche FA, Richardson HE, Harvey KF. "Upstream Regulation of the Hippo Size Review Control Pathway". *Curr Biol*. **2010**; Vol. 20: pR574-R582
14. Al-Greene NT, Means AL, Lu P, Jiang A, et al. "Four jointed box 1 promotes angiogenesis and is associated with poor patient survival in colorectal carcinoma". *PLoS One* **2013**; Vol.29: e69660
15. Rock R, Heinrich AC, Schumacher N, Gessler M. "Fjx1: A Notch-Inducible Secreted Ligand With Specific Binding Sites in Developing Mouse Embryos and Adult Brain". *Dev Dyn*. **2005**; Vol.234: p602-12
16. Matis M, Axelrod JD. "Regulation of PCP by the Fat signalling pathway". *Genes Dev*. **2013**; Vol.27: p2207-20
17. Roudkenar MH, Kuwahara Y, Baba T, Roushandeh AM, et al. "Oxidative Stress Induced Lipocalin 2 Gene Expression: Addressing its Expression under the Harmful Conditions". *J. Radiat. Res*. **2007**; Vol.48: p39-44
18. Adiyanti SS, Loho T. "Acute Kidney Injury (AKI) Biomarker". *Acta Med Indones*. **2012**; Vol.44: p246-55
19. Vaidya VS, Shankar K, Lock EA, Bucci TJ, et al. "Renal injury and repair following S-1,2 dichlorovinyl-L-cysteine administration to mice". *Toxicol Appl Pharmacol*. **2003**; Vol.188: p110-21

20. Norman J. "Fibrosis and progression of Autosomal Dominant Polycystic Kidney Disease (ADPKD)". *Biochim Biophys Acta*. **2011**; Vol.1812: p1327-1336
21. Bolisetty S, Traylor AM, Kim J, Joseph R et al. "Heme Oxygenase-1 Inhibits Renal Tubular Macroautophagy in Acute Kidney Injury". *J Am Soc Nephrol*. **2010**; Vol. 21: p1702–1712
22. Romagnani P, Kalluri R. "Possible mechanisms of kidney repair". *Fibrogenesis Tissue Repair*. **2009**; Vol.2: p3

In appendices:

23. Lancaster MA, Gleeson JG. "Cystic kidney disease: the role of Wnt signaling". *Trends Mol Med*. **2010**; Vol.16: p349-60
24. Kohan DE. "Progress in gene targeting: using mutant mice to study renal function and disease". *Kidney Int*. **2008**; Vol. 74: p427–437
25. http://www.ruf.rice.edu/~rur/issue1_files/norman.html (11-4-2016)

Picture frontpage:

<http://pkdcharity.org.uk/about-adpkd/just-diagnosed/i-want-to-know-more> (5-11-2015)

Appendices

1 PCP pathway

Noncanonical/Planar Cell Polarity

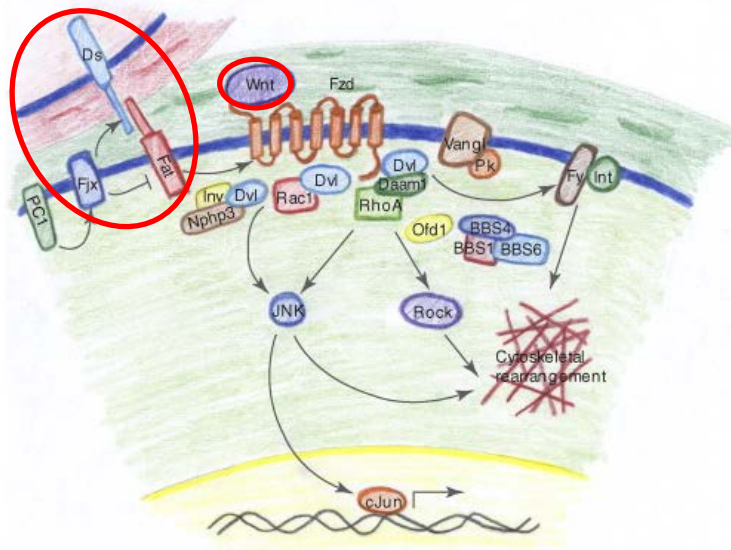


Figure 17. The PCP-pathway, showing both regulation possibilities outlined in red: activation by Wnt can induce signalling, while Fjx1 via the Fjx1/Fat/Ds complex also can induce signalling.²³

2 Background mouse models

In this experiment C57Bl/6J mice are used. *Fjx1*^{-/-} mice have a germ line mutation, while the *Pkd1* KO was induced in the kidneys of adult mice, using the Cre/Lox system.

In the Cre/Lox system a gene of interest is placed in-between two LoxP sites (a part of the DNA containing a specific sequence). These sites can be cut through the enzyme Cre recombinase, which is transcribed to be an inactive form. This will be activated by tamoxifen. This results in an excision of the gene of interest at a desired time point, as shown in figure 18.²⁴

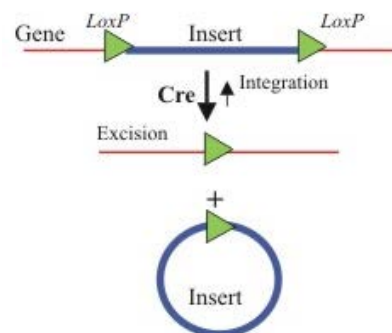


Figure 18. Cre/Lox system. Cre cuts LoxP sites, herewith excising a gene of interest.²⁵

To induce the *Pkd1* KO, adults of 13 or 14 weeks old were given tamoxifen (5 mg/mouse by oral gavage) for three consecutive days. After one week, mice were given an intraperitoneal injection with DCVC to induce renal injury (15 mg/kg, dissolved in PBS) or PBS as a control. At several fixed time points after injection, namely 1, 2, 5 and 10 weeks, tissue was obtained. Tissue was also obtained when the blood urea level exceeded 25mmol/l, because this indicates severe kidney failure and therefore the mouse was sacrificed. These time points were established in earlier experiments, described in Happé et al. (2009).¹¹ All groups consist of 6 mice per time point, which creates a total amount of 240 mice for this study. An overview is given in figure 19.

To rule out any influence of the lox-sites, the *Pkd1* gene is also floxed in the wild type (compared to the *Pdk1* KO model). No Cre enzyme is present, avoiding excision of the gene.

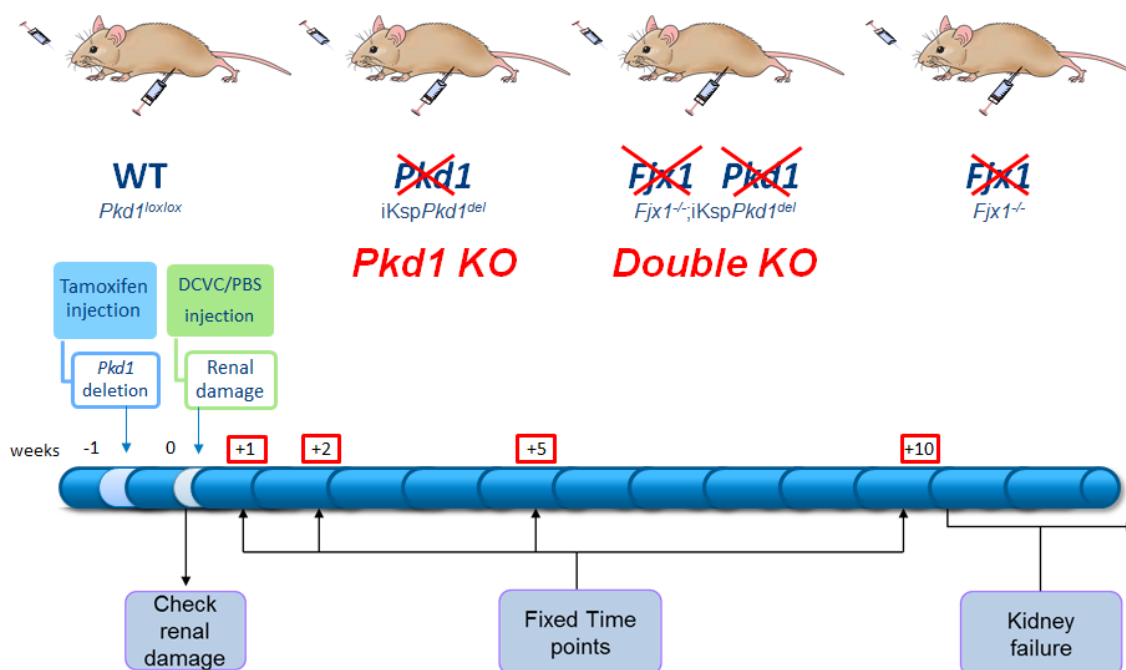


Figure 19. Overview of the mouse models and time points.

3 Preliminary results

From the tissue samples some data has already been collected, for example a calculation of the two kidney-weight/body-weight ratio, blood urea level and age at point of sacrifice. These data resulted in preliminary results, of which two are important.

Firstly, it's been confirmed that the damage induced by DCVC is able to cause a faster development of the disease in the *Pkd1* KO mice compared with the PBS injected group. But in the *Fjx1*^{-/-};*Pkd1* KO genotype the kidney failure occurs in a comparable time for the DCVC injected mice and the PBS injected mice (which is also the same as for the *Pkd1* KO mice injected with PBS, see figure 20).

These findings suggest that the *Fjx1*^{-/-};*Pkd1* KO model has a faster or more effective response to the damage which allows them to survive longer. Therefore *Fjx1* seems to be involved in tissue repair. Secondly, the two kidney weight/body weight ratio shows a difference in the phenotypes: the *Fjx1*^{-/-};*Pkd1* KO model shows enlarged kidneys compared to the *Pkd1* KO model. Therefore *Fjx1* seems to be involved in tissue size control.

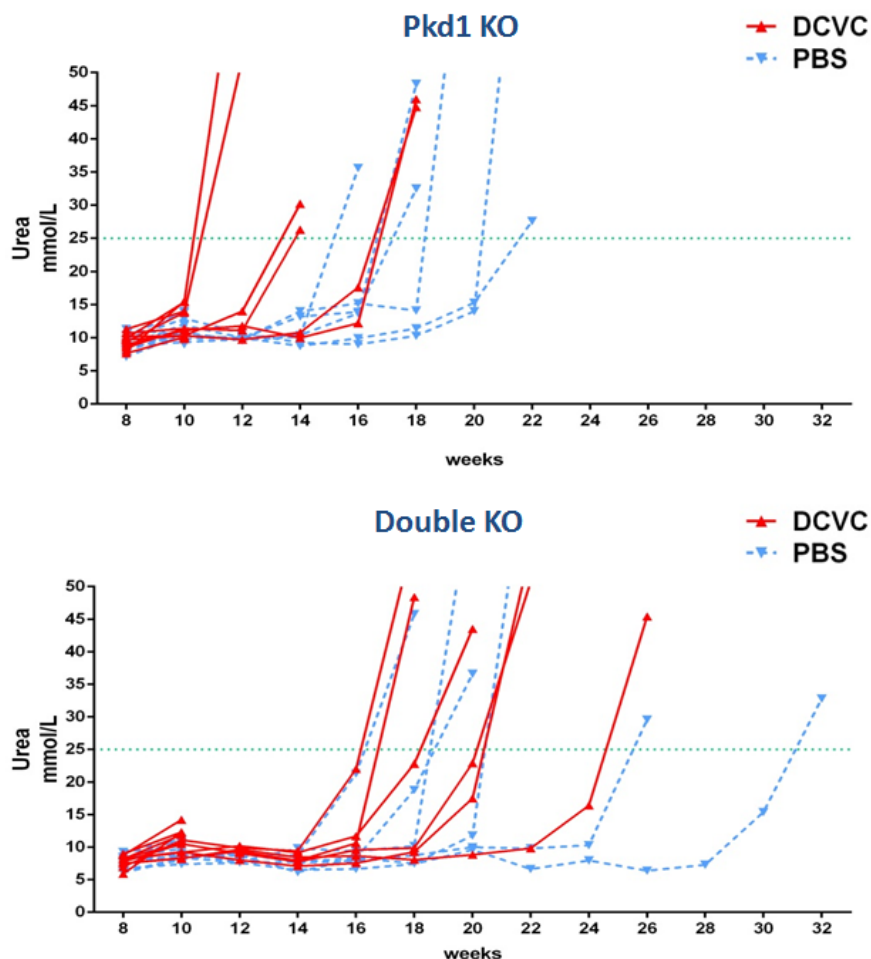


Figure 20. Comparison of renal failure. In *Pkd1* KO mice renal failure in DCVC-treated mice is reached at a significant younger age compared to the PBS-treated mice (median 19 weeks compared to 14 weeks). For the *Fjx1*^{-/-};*Pkd1* KO mice this difference between DCVC- and PBS-treated mice is not seen (median 21 weeks compared to 20 weeks). The delay of renal failure in DCVC-treated *Fjx1*^{-/-};*Pkd1* KO mice compared to DCVC-treated *Pkd1* KO mice is significant.